IEEE Access
Multidisciplinary ⋮ Rapid Review ⋮ Open Access Journal

Received 3 June 2022, accepted 29 June 2022, date of publication 7 July 2022, date of current version 18 July 2022.

Digital Object Identifier 10.1109/ACCESS.2022.3189002

RESEARCH ARTICLE

An Efficient LoRa-Enabled Smart Fault Detection and Monitoring Platform for the Power Distribution System Using Self-Powered IoT Devices

GEORGE Y. ODONGO[1,2], (Graduate Student Member, IEEE), RICHARD MUSABE[1], DAMIEN HANYURWIMFURA[1], AND ABUBAKAR DIWANI BAKARI[3]

[1]African Centre of Excellence in the Internet of Things (ACE-IoT), College of Science and Technology, University of Rwanda, Kigali, Rwanda
[2]Department of Computer Science, Egerton University, Nakuru 20115, Kenya
[3]Department of Computer Science and Information Technology, State University of Zanzibar (SUZA), Tunguu, Zanzibar 31308, Tanzania

Corresponding author: George Y. Odongo (godongo@egerton.ac.ke)

This work was supported in part by the University of Rwanda through the African Centre of Excellence in Internet of Things (ACE-IoT).

ABSTRACT Transient stability and supply disturbances are common yet unwelcome phenomena in power distribution systems, particularly in sub-Saharan Africa. The growing demand for greater reliability and dependability in power delivery has aroused the interest of researchers and renewed the pursuit of advanced technological solutions for fault detection and location determination at medium and low-voltage levels. The length of the distribution network typically ranges from hundreds to thousands of kilometers. In this regard, the management of distribution networks, including the identification of faulty segments, is a significant recurrent challenge facing power-system operators. With the ever-expanding distribution network and regulatory demands for service reliability, the challenge for network operators is daunting. However, the deployment of IoT technologies in the energy distribution infrastructure would significantly accelerate the detection and location of faults, thus transforming the electricity delivery service into one that is responsive, communicative, attractive, and robust. This study proposes, designs, and implements a reasonably priced LoRaWAN-based IoT platform for monitoring distribution networks. The study was conducted in Nakuru County, Kenya on an actual and active distribution network owned and managed by Kenya Power Company. Experimental results showed that a trigger is generated at the network-monitoring center in about 100 ms of the occurrence of a fault on the distribution network, thus enabling quick, prompt, and immediate commencement of reparative action. Furthermore, practical evaluation has shown that this platform is well adapted for the context of developing countries where budgetary constraints and cost prohibitions hinder the upgrade of the legacy grid into fully-fledged smart entities.

INDEX TERMS Distribution transformer, fault-monitoring, IoT, LoRaWAN, power distribution system.

I. INTRODUCTION

The legacy power distribution grid that is still widely in use was never built to enable two-way communication, and neither was it made with the ability to facilitate real-time monitoring by the service provider [1], [2]. Whereas electricity generation and transmission are meticulously monitored by highly advanced and computerized technologies, the distribution segment lacks a comparable level of sophistication [3]–[6]. Because there is no automated means of monitoring power delivery to consumers, this lack of feedback impedes efficient management of the power distribution grid [7]. In the event of a power failure, the service provider remains completely oblivious to the fact, resulting in a hue

The associate editor coordinating the review of this manuscript and approving it for publication was Rui Li.

and cry from the affected consumers. This lack of feedback also delays the initiation of reparative and restorative activities and interrupts the revenue stream for the power system operator (PSO) [8], [9]. In response to this issue, service providers have had to employ strategies that attempt to keep them informed about problems on the distribution side of the network. In Kenya, for instance, Kenya Power Company Plc., the lone purveyor of electricity, encourages its clients to communicate with the company through telephone calls whenever they experience an interruption in power delivery. The power system operator provider has set up call centers and publicized its telephone and email contacts to be used for this purpose [10]. In order to ascertain the loss of power, Kenya Power clusters the telephone calls according to the areas they originate from, makes a guess at the probable location of the problem, and then sends out a service crew team to find and repair the fault [11]. This arrangement, however, ambitiously assumes that the client is constantly monitoring the power supply in the affected premises and that the customer is very conversant with troubleshooting the power network. However, even with this arrangement, the time it takes the service provider to learn about an active fault is inordinately long, resulting in prolonged episodes of power blackouts. Every year, Kenya Power customers experience up to 25,000 minutes of power outages [12]. For a growing economy with ambitious goals for the future, this is untenable.

As of June 2021, Kenya had an installed capacity of about 2,813 megawatts generated from various sources as follows: about 29.4% was hydro power, 29.4% was geothermal, 26.6% was thermal, and 11.8% was wind, with solar and biomass closing the list at 1.8% and 1%, respectively [13], [14]. Fig. 1 is a graphical representation of Kenya's energy generation mix. This energy is distributed to about 7.5 million customers through a distribution and transmission network consisting of about 74,608 kilometers of electric lines.

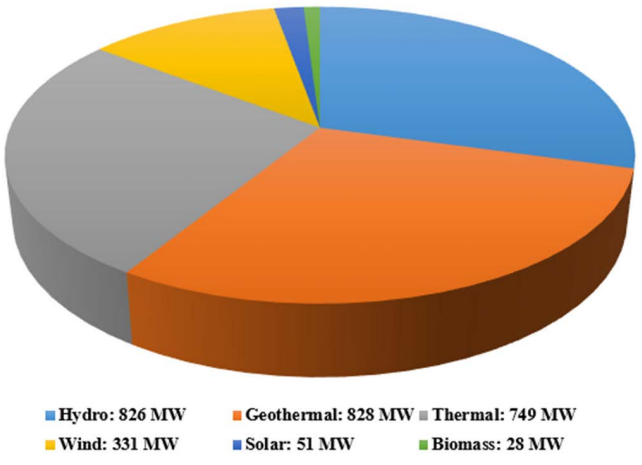

FIGURE 1. Kenya's energy generation mix.

Disturbances in the power system are not entirely avoidable. In such a vast and expansive system with so many variables and factors at play, one thing or the other will at any one time go wrong, and when this happens, it is important that the incident be immediately brought to the attention of the service provider [15]. The greater the time it takes to become aware of and mitigate a fault, the greater the ensuing damage to adjacent equipment and infrastructure, resulting in even more catastrophic failures and costly reparation.

In developed economies, this problem is being addressed by the gradual rollout of the Smart Grid (SG). Due to its ability to integrate power, data, and message exchange to fashion an efficient energy system, the smart grid is seen as a potential solution to the lack of feedback from the electricity grid [3], [16], [17]. This solution, however, is unappealing in developing countries due to the prohibitive costs involved [16]–[19].

A. RELATED LITERATURE

The goal of this section is to conduct a critical review of related works for fault monitoring on power distribution systems, as well as techniques for powering IoT devices in such deployments. An extensive review of published scholarly works reveals that a variety of approaches have been proposed in the literature to address the fault detection and location discovery problem, including Petri nets [20]–[23], fuzzy-based methods [24]–[28], artificial neural networks [29]–[31], expert systems [32]–[35], and analytic models [36]–[38]. Although the aforementioned approaches have some very strong points in some respects, they also display certain weaknesses. For example, it is difficult to establish and maintain a knowledge base in expert systems; artificial neural networks are lacking in terms of interpreting reasoning results; fuzzy theory employs membership functions and fuzzy rules that are susceptible to subjective tendencies; and petri-based methods have poor adaptability and difficulties in online modeling.

In [39], a study that focused on fault diagnosis in power transformers and the role of IoT in power maintenance is reported. Thirty faulty transformers were selected, with 20 of these being used for training while the other 10 were used for testing. For communication, the General Packet Radio Service (GPRS) was used. The researchers studied the rate of accurate detection of the proposed IoT-based power transformer fault analysis method. It was reported that a training error of less than 0.01% was observed, with the model accurately identifying 95.6% of the faults, including those not used in training. In [40], a model that exploits the Ohms law to detect the fault location is proposed. The model enabled technicians to find the precise fault location and assisted service personnel in removing persistent faults, thus reducing the occurrence of faults and minimizing the time of power outages. The system used an Arduino to analyze the distances of the fault incidents with the help of software developed for the purpose. The fault location was relayed using a Wi-Fi module. In [15], a remote IoT surveillance and fault prediction arrangement grounded on custom-made software-defined networking (SDN) is proposed. The methodology, described as an evolution into a smart grid deployment, was based on a tailored software-defined network.

The proposed architecture showcased an efficient method of handling imminent interruptions and faults in the power system via reasonably priced and dependable frameworks that predict and deliver live condition monitoring indicators. A prediction accuracy of about 96.1% was attained.

A novel method for precisely locating faults that exploits the various measurements obtainable is proposed in [41]. To determine the closest position to the culpable site, the devised method iteratively estimates the fault site. The lines connecting to the chosen site are then scanned in order to pinpoint the problem. A simulation test was conducted on an actual distribution grid, and various failure situations were considered to appraise the performance of the suggested technique. The upshot of this appraisal was that the method is accurate and robust even when the measured data is questionable and it reliably manages measurement mistakes. A novel smart current and voltage observation method is suggested in [41]. The system monitored a 3-phase power grid using an open-source microcontroller, which read currents and voltages from sensors. The readings were then sent wirelessly to an Android application for analysis. The system enabled the monitoring of some basic voltage and power quality aspects. In [42], an algorithm that uses zoning in the Power Distribution System (PDS) is proposed. It communicated with a cloud server through an edge node and delivered time-harmonized current quantities. A database was used to record all fault incidences that occurred in the power distribution system. Results showed that the procedure was successful at localizing the faults in all the test cases conducted.

A mature system that has been extensively used for fault detection for several decades is Supervisory Control and Data Acquisition (SCADA) [2], [43], [44]. It is not only used in the power industry but also in several other industrial settings, such as manufacturing, water management and treatment systems, and oil and gas facilities. SCADA is basically a centralized system that monitors and controls a given production environment by gathering relevant data and sending back commands to control certain aspects of the process [45]. Fig. 2 displays the fundamental components of the SCADA system. Due to the length and breadth of the distribution network, it is often not practically possible to run SCADA over it because of the exorbitant installation costs. Such an installation would cost hundreds of thousands of dollars, canceling out any potential gains achievable from such action. It is for this reason that many service providers have shied away from a SCADA-monitored distribution grid [46].

In [47], phasor measurement units (PMUs) have been described as being an integral part of a sophisticated technology for advanced measurement and monitoring of energy transmission and distribution. In contrast to other existing grid measurement methods, PMUs can provide highly accurate and synchronized real-time measurements via Global Positioning System (GPS) signals [47]–[49]. PMUs are typically installed at power substations and work by measuring the amplitude of the voltage and the current at preselected points using current transformers (CTs) and potential

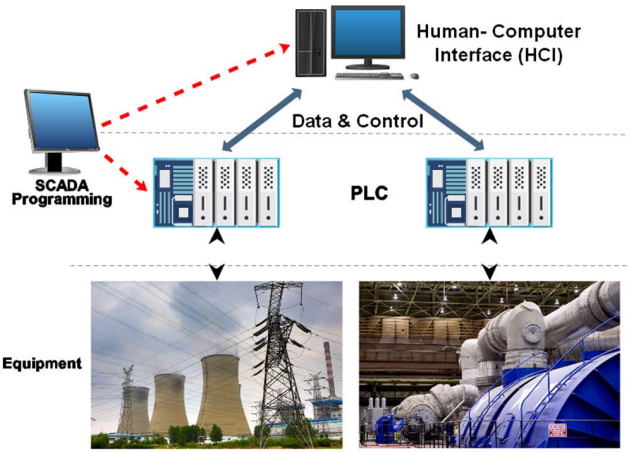

FIGURE 2. Main components of a SCADA system.

transformers (PTs). The phase of the measured quantities along with their time-synchronized signals are also taken and sent to a phasor data concentrator (PDC) for onward transmission to the control center for further analysis. PMUs are widely used and have been extensively integrated into the transmission and distribution grids. This technology is, however, very expensive and is seldom used on the distribution network.

A suggestion was made in [11] to use smart meter measurements to detect the location of distribution grid faults using a state-approximation-based technique. The suggested technique uses the variable weighting matrix identification method to discover the faulted section. The approach is simple to implement algorithmically and does not require the use of a fault type [11]. An assumption is made that the currents and voltages measured as the fault develops are accessible by the main substation.

Numerous research has also been conducted on the adoption of intelligent algorithms and machine learning methods for power fault detection and analysis. In [50], a proposal is made to detect faults using a Fuzzy Logic Controller (FLC) and to identify the fault location, an Adaptive Neuro Fuzzy Inference System (ANFIS) is suggested. The study focused on how the distribution grid incidences can be detected, identified, and located. A fuzzy controller was incorporated into the system to recognize the different kinds of faults upon their occurrence. The model was developed in MATLAB and the results showed that ANFIS attained an accuracy of 51% for identification and 93% for location.

Other researchers have also extensively reported on LPWANs[51] compares the two main technologies in the LPWAN space against GPRS. The study found that, as compared to the coverage area of ZigBee and Wi-Fi, LPWANs enable considerable connections covering long distances at low cost and are devoid of the requisite maintenance. In [52], a study seeking to understand the abilities and shortcomings of LoRa technology in terms of its throughput, coverage, and scalability is reported. The study used a combination of

measurements from a real-world citywide LoRa deployment and high-fidelity simulations to obtain and analyze the measurement data collected. The results showed that within a radius of about 15 kilometers, three gateways were able to sufficiently cover the area and provide connectivity to about 1,000,000 end devices. The study illustrated the resilience of LoRa, especially in a dense urban environment. In [53], a study on the performance of an IoT application based on LoRaWAN is reported. The experiment sought to obtain insight into the packet loss, RSSI, and SNR values between the transmitting device and the receiving one. Experimentation results showed that when the spreading factor is high, LoRa end devices tend to provide greater immunity against signal fading and multi-path fading.

IoT has today made it possible for miniature, alternatively-powered devices to be embedded in the environment, monitoring a diverse range of quantities in various fields such as agriculture, security, manufacturing, environmental monitoring, healthcare, transportation, just to name a few. This embedding has concomitantly created a need for innovative ways to power these embedded devices. Consequently, the term ''energy scavenging'' has become relevant in this context. Energy exists in the environment in many different forms and can be harvested for use in low-power-demanding applications [54]. In [55], various latent energy sources in the environment are identified, such as chemical, mechanical, acoustic, solar, and radio frequency (RF). The harvesting of ambient energy coupled with the usage of rechargeable batteries for energy storage is beneficial for Wireless Sensor Network (WSN) operations, opines Dhananjaya [56]. His work further observes that WSNs require energy harvesting to avoid frequent battery replacement and associated costs. Energy harvesting enables on-site charging of rechargeable batteries, which may be cycled hundreds of times before losing their capacity. The battery's life may be prolonged practically forever with the right technology and energy management. As observed in [57]–[59], long-term deployment of IoT devices necessitates some form of energy harvesting. In particular, photovoltaic (PV) cells have been identified as a feasible, low-cost, and long-term energy source for IoT sensors.

B. IoT, LPWAN, LoRa®, AND LoRaWAN®

''IoT,'' which is an abbreviation for ''Internet of Things,'' is a notion that promulgates the idea that millions of independent, ubiquitous, internet-enabled devices can spontaneously and autonomously initiate connectivity with other similarly connected devices and share information at any time, any place, and anywhere [60], [61]. With the widespread adoption of IoT solutions across a wide range of domains [62], the focus has shifted to how these IoT devices can connect from remote and distant locations given that they are battery-powered and severely resource constrained [63], [64]. It is from this perspective that LPWAN, short for low-power wide-area network, comes into play. The term LPWAN refers to communication protocols and technologies that embrace two unique properties: one, they have an enviably small energy demand; and two, they possess the ability to communicate over distances tens of kilometers apart. Due to their low energy demands, LPWAN-compliant devices have an uncanny ability to run for several weeks, maybe even years, on nothing but low-capacity battery cells. As opposed to wireless WANs, which are designed to carry more data using more power, LPWANs have a low data rate that is typically less than 50 kbit/s per channel [65]. The reach of LPWANs varies but can be greater than 15000 meters depending on the specific technology, with payloads of up to 1000 bytes [52], [66]. As such, the term LPWAN does not refer to a specific technology but is a generic term used for various long-reach but low-power-consuming networking technologies that come in various shapes, sizes, and flavors [67]. LPWANs can be proprietary or open-standard, and they can use licensed or unlicensed frequency bands [68]. Some examples of LPWAN compliant technologies include ZigBee, SigFox, Nwave, RPMA, Ingenu, LoRa, NB-IoT, LTE-M, and NB-Fi.

LoRa® is an abbreviation for ''Long Range'' and is the name of a physical layer proprietary LPWAN technology founded on the spread spectrum modulation technique that is plagiaristic of the Chirp Spread Spectrum (CSS). Because of its low power, low bandwidth, and long range capability, LoRa has emerged as a boon for the IoT, particularly for wide-area data haulage [69]–[73]. LoRa devices offer fascinating characteristics for IoT use cases that include long-range communication, low power demand, and secure data transfer. It was developed by Cycleo SAS about a decade ago, and later it (Cycleo SAS) was acquired by Semtech [74], [75]. Since then, Semtech has successfully leveraged the wide area connectivity capabilities of LoRa, so much so that today more than 65 million devices across more than 120 countries are using LoRa [76], [77]. LoRa technology, whose physical layer was patented in July 2014, is favored for many reasons. Not only is it long range and low cost, but it makes judicious use of scarcely available power, giving it the ability to operate for many weeks, possibly years, powered by nothing but tiny energy reservoirs [62], [64], [70].

From an architectural point of view, a typical LoRa deployment can be divided into four distinct sections [70], as shown in Fig. 3. A LoRa network can allow an assorted array of embedded sensors to transmit information to a central gateway, which then forwards the same to an application server via a network server. The end devices, otherwise known as motes or nodes, are ordinary objects equipped with low-power communication devices. The gateways are the devices that receive and transmit data from and to the motes. The gateways themselves must be connected to the network servers via some kind of backhaul network connection [66], [78]. The network server is the workhorse of the network. The network server manages the gateways and allows the end devices to securely communicate with the cloud. It has all the intelligence to perform security checks, remove duplicate packets, acknowledge packets received

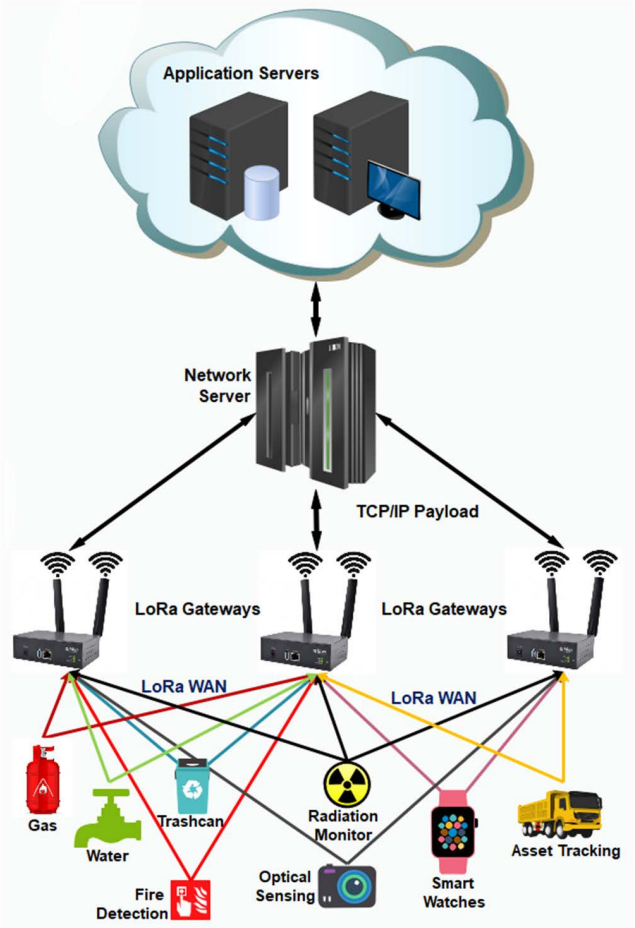

FIGURE 3. Architectural layout of a LoRaWAN deployment.

from the gateways and channel packets received to the relevant application server. The application is just some software executed on an Internet server.

LoRaWAN is an implementation of the adaptive data rate (ADR) algorithm that regulates the communication speed for each node individually. The terminal nodes are permitted to transmit data using any ADR speed over any available channel at any time. Specific rules, however, must be followed, one of which being that the end devices are required to change the channel haphazardly for every broadcast. This ensures the availability of a variety of frequencies for data transmission. The end nodes are further obligated to observe restrictions on transmission duty cycles defined by the range specification.

The architectural framework of LoRaWAN comprises four major components, as shown in Fig 3. These four components are the end nodes; the gateway; the network server; and the application servers. This framework shows how LoRa and LoRaWAN allow dense but widely spread-out networks of edge devices to be connected, thus enabling data collection and monitoring from thousands of nodes in a manageable way. The end nodes are the devices situated at the network boundaries and will usually be equipped with sensory capabilities, the type, design, and function depending on the specific use case.

Customarily, a low-powered microcontroller is used to build end nodes. This gives the nodes the ability to linger on in the environment for many months or years without requiring regular servicing. They will usually be fitted with a means of communication that requires minimal power. The gateways receive and forward data from the end nodes and can therefore be thought of as bridges between the nodes and the network. Because of its primary role in the network, the gateway can also be considered a packet forwarder [70]. The network server amalgamates all the data they receive from the various gateways and uploads it to the application server. Finally, the data collected from the field by the different end nodes must be interpreted either visually or analytically. This role is played by the application server. In addition, specific actions or triggers may be initiated as a consequence, such as a notification service to inform the resident engineer when a potential issue has arisen, or the mere opening of a window or turning on rainwater pumps for agricultural use cases.

LoRa functions in the unregulated and free-to-use unlicensed Industrial, Scientific, and Medical (ISM) radio bands that are sections of the radio frequency spectrum retained internationally for ISM purposes [69]. The ISM radio bands assigned for use in specific countries differ from one to another but are either 433 MHz, 868 MHz, or 915 MHz. In the US, for instance, the frequency sub-band used is 915 MHz, while in the EU, 433 MHz or 868 MHz sub-bands are used. Other regions of the world will also have specific frequency allocations as set by regional regulatory agencies [79]. Even though LoRa functions in the free and unlicensed ISM radio bands, there are regulations on how much power it can transmit, its duty cycle, and sometimes the bandwidth. For instance, in the EU, a duty cycle limit of 1% per sub-band per hour is specified.

LoRa modulation characteristics are premised on three configurable properties that remarkably alter its performance: the coding rate (CDR), the spreading factor (SF), and the bandwidth (BW). The bandwidth is the breadth of the spectrum that a chirp occupies. LoRa provides for a tripartite bandwidth setting of either 125 kHz, 250 kHz, or 500 kHz [80]. The chosen setting will determine the rate at which the transmitter sends data to the receiver. The spreading factor is a significant parameter that determines how many chirps are encoded per symbol and hence the modulation rate. The spreading factor (SF) is chosen such that $SF \epsilon \{7, 8, 9, 10, 11, 12\}$. The chirp rate ($CPR$) is the first derivative of the chirp frequency. Equation (1) shows how the three parameters are related.

$$CDR = {BW}/{2^{SF}} \tag{1}$$

where CDR stands for coding rate, SF stands for spreading factor, and BW stands for modulation bandwidth. Equation (2) shows how the SF, BW, and CDR influence

the bitrate (BR).

$$BR = SF \cdot \frac{BW}{2^{SF}} \cdot DR \tag{2}$$

where SF stands for spreading factor, BW stands for modulation bandwidth, and CDR stands for coding rate. The coding rate (CDR), expressed as a fraction, denotes the quantity of transmitted bits that carry the essential information. The higher the coding rate value, the lower the effective data rate since a data payload is of a prescribed size. LoRa can be configured for four different coding rates as shown in (3).

$$CDR = \frac{4}{(4 + EC)} \tag{3}$$

where EC is a value in the set $\{1, 2, 3, 4\}$, and describes how sensitive a receiver should be in detecting and correcting amending mistakes in the sent message. Using (3), it is found that the coding rate can be one of the following$\{4/5, 4/6, 4/7, 4/8\}$ [81].

There are three classes of end devices defined in the LoRaWAN specification, viz., classes A, B, and C. A class A device has extreme savings on the available power since every transmit session is initiated by the end-node rather than by the gateway. As such, the end nodes can create and observe a transmit schedule with the least duty cycle. After an end node initiates an uplink, an optional downlink opportunity is made available to the gateway to transmit its own frame in case there is a need for such [82]. With a class B device, however, the end node must first synchronize its internal clock with that of the gateway using beacons received from the gateway. During this process of synchronization, the gateway can create a data transmission and synchronization schedule with the nodes. Each class B device will therefore utilize the allotted time to transmit uplink frames. Class C devices are perpetually paired with the gateway. This arrangement assumes that power is continuously available and is, in fact, unlimited. Fig. 4 compares the various classes of devices in terms of their communication latency and how efficiently they utilize energy.

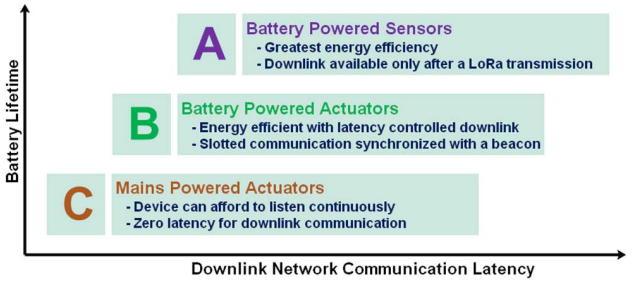

FIGURE 4. A comparison of Class A, Class B and Class C devices.

Most off-the-rack LoRa end nodes are built to comply with the Class A specification. Because LoRa Class A devices use a channel access method similar to ALOHA, there is a small probability that two frames sent by two end nodes using the same spreading factor will collide [70], [83]. However, since a LoRa broadcast has an infinitesimal duty cycle, the probability of frame contention is considerably low. But in Classes B and C, the synchronization that precedes a transmission renders the communication channel collision-free [84].

Whereas LoRa is a description of the lowest physical layer, the higher layers were initially not defined. This void necessitated the creation of LoRaWAN, which is one of a number of protocols that have been created to define the higher layers of the protocol. It can obtain real-time data from various objects in the environment and is an open, secure, and interoperable worldwide standard for wireless communication. It acts principally as a network layer routing protocol that manages the manner in which end-nodes and gateways communicate, but it is actually a MAC layer protocol based on the cloud. The LoRaWAN standard was proposed by the LoRa Alliance, which is a global association whose members' ecosystem developed and maintains the LoRaWAN protocol. The LoRa Alliance, created in 2015, is an open, not-for-profit association with over 500 members who actively support and maintain the LoRaWAN protocol, thus ensuring interoperability of all LoRaWAN products and technologies. Fig. 5 shows the LoRa protocol stack. At its lowest level, the physical layer (PHY) is found, which is where LoRa is domiciled. Then, above it, we have the media access control (MAC) layer, whose function is to eliminate duplicate receptions, assign frequencies, spreading factors, and data rates to the devices, among other things. The application layer handles the data encryption and decryption as well as encoding and decoding.

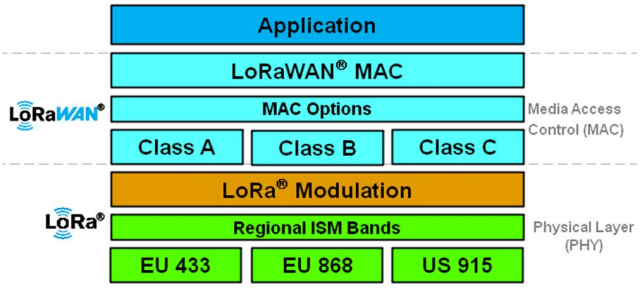

FIGURE 5. The LoRaWAN protocol stack.

C. TYPES OF FAULTS

A fault on the electric grid is the sudden and possibly cataclysmic departure of voltages and currents from their rated values that affect usual operations. The equipment of the power network, including the conductor cables, ordinarily carries voltages and currents that guarantee the safe operation of the system. However, when faults ensue, they cause extraordinary current flow streams that may result in the impairment of adjacent equipment [42].

Faults in the electrical power system can be either symmetrical or non-symmetrical. Symmetrical faults, also known as balanced faults, are very severe. Nevertheless, their occurrence is quite rare. A balanced fault can appear as a line to line

to ground (L-L-L-G) or a line to line to line (L-L-L), as illustrated in Figs. 6 (a) and 6 (b). Symmetrical faults are estimated to have an occurrence frequency of between 3 and 6%. Since symmetrical faults leave the system in a balanced state, such faults usually result in colossal destruction of the power equipment [85].

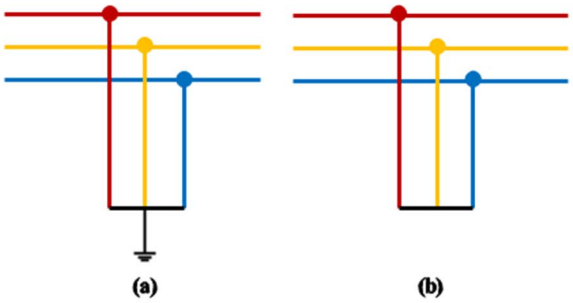

FIGURE 6. Symmetric faults (a) Line-to-Line-to-Line-to-Ground (b) Line-to-Line-to-Line.

On the other hand, non-symmetrical faults, also known as unbalanced faults, are less severe yet extremely common. When the impedance values of each phase differ, the current flows in those phases are dissimilar. This state is what is referred to as an imbalance in the system. There are three main manifestations of non-symmetrical faults, namely double line to ground (LL-G), line to line (L-L) and line to ground (L-G) faults [86]. Line to ground fault (L-G) is by far the most frequent type of fault in this category and accounts for 65 to 70% of fault manifestations [85]. Fig. 7 is a diagrammatic representation of non-symmetric faults.

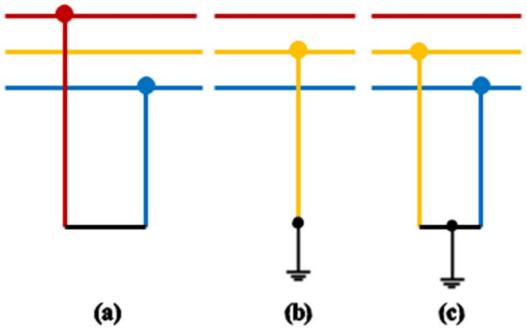

FIGURE 7. Non-symmetric faults (a) Line-to-Line (b) Line-to-Ground (c) Line-to-Line-to-Ground.

D. ORGANIZATION

The remainder of this paper is organized as follows: In Segment II, we will discuss the materials and methods that have been used in this study. Segment III presents the experimental results. In Segment IV, a discourse on the significance of the finding is undertaken, and in Segment V, the study is concluded. All the abbreviations used in this work are explicated in Table 8.

II. MATERIALS AND METHODS

A. ABOUT THE STUDY LOCATION

This study was conducted in Nakuru County in the East African country of Kenya. Nakuru is located 189 km north of the city of Nairobi and has an altitude of 2217 meters above sea level. Kenya Power (KP) Company Limited has created eight administrative regions, namely: Central Rift, North Rift, Mt. Kenya, North Eastern, Coast, South Nyanza, Nairobi, and Western regions. Njoro Sub-county falls under the Central Rift Region, which has about 1.6 million subscribers.

Nakuru is host to several factories and industries that give the area significant economic importance. The operations of all of these factories rely on a stable supply of electrical energy. As a popular tourist destination, Nakuru is host to several hotels and resorts that receive its many visitors. All these places need to be powered reliably and continuously.

B. SYSTEM DESIGN AND CONSTRUCTION

The proliferation of miniature sensors that survive on limited energy sources has given impetus to this study's goal of actualizing a LoRaWAN sensor network to monitor the power distribution grid [87]. When constructing IoT devices, the overall goal is to construct devices that will conserve as much power as possible. The designed system comprises the cloud application server, network server, LoRa gateway, and field deplorable sensors. Table 1 outlines the various components that were used to build the platform.

The Arduino microcontroller was preferred for this work due to its low power consumption and its versatility in terms of the projects that can be undertaken through it. Along with the little power-consuming hardware, the algorithm that it was developed to run is also power-conserving. Fig. 8 shows a flowchart of the algorithm executed by the microcontroller. The algorithm departs from the conventional ''polling'' technique. The polling technique uses sensors that are configured to continuously take readings at a regular set interval and, as such, is energy-hungry. In contrast, our method uses ''interrupts'' instead to alert the microcontroller unit of an abnormal situation in the quantity being observed. This means the Arduino microcontroller can be in a state of ''deep sleep'' most of the time. In a deep sleep state, the microcontroller uses minimal power as opposed to an always-on operation, which is power-consuming. The device is configured such that when an interrupt is detected, the microcontroller wakes up from its state of ''deep sleep'' and sends an alert to the monitoring and control center, informing them of an anomaly. This mode of operation is highly energy efficient, especially since we desire the IoT device to conserve as much power as is practically possible without compromising its ability to operate.

1) GATEWAY SETUP AND CONFIGURATION

The RAK7258 Micro Gateway was selected for this work. The gateway with Power-over-Ethernet (PoE) capability

TABLE 1. Bill of materials for the fault detection platform.

COMPONENT	PURPOSE
Arduino MEGA 2560 Rev3	Microcontroller unit
Dragino LoRa Shield SX1278 chip (868Mhz)	LoRa transceiver on an Arduino shield form
GSM/GPRS SIM900 Module	Global Positioning System (GPS) location information
RAK7258 Micro Gateway	LoRaWAN Gateway
Real Time Clock DS3231	Precise real-time keeping
Solar Panel (5V, 3.5W)	Solar energy harvesting
STC013 100A:5mA	Current Transformer
TP 4056 charge module	DC-to-DC Voltage Booster/ Solar Charge Controller

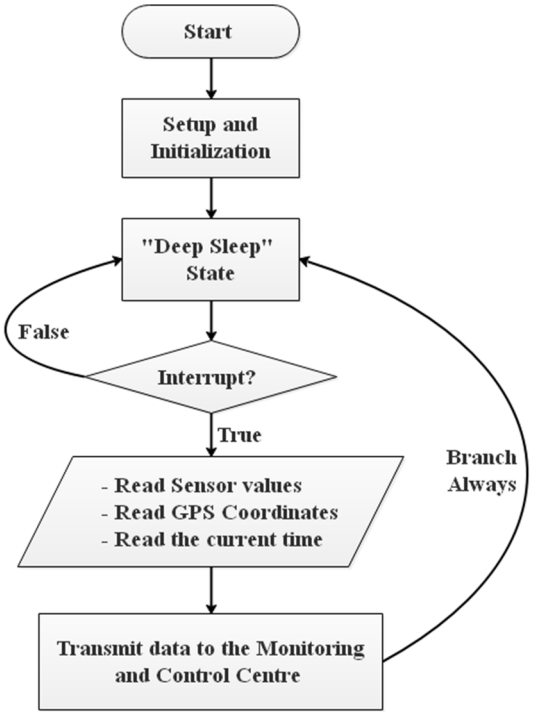

FIGURE 8. A flowchart of the fault-monitoring algorithm.

is managed and configured through the open wireless router (OpenWRT) user interface. Data destined for the local server is relayed by means of the MQTT protocol. Given the size and format of the messages, MQTT is appropriate for use in relaying the messages to the server [88]. The data from the sensing devices is aggregated and forwarded to the network server. The RAK7258 Micro Gateway is a full-featured, eight-channel gateway that uses IP to connect to the wireless LoRa network. It is powered by a 12V-1A DC power supply and operates at a frequency of 868MHz with a listed minimum receiver sensitivity of −142dBm. Packets are relayed to the local server via an Ethernet backhaul.

The gateway message protocol (GMP) is used to send LoRaWAN messages over the wireless interface.

2) EMBEDDED ELECTRONIC MONITORING DEVICE

The Embedded Electronic Monitoring Device (EMMD) was constructed using the open source hardware Arduino MEGA 2650 Rev3 microcontroller (MC). Fig. 9 shows the layout of the selected Arduino microcontroller along with its various parts. The microcontroller board was programmed to read from the current transformers (CT) attached to the outbound supply lines of the distribution transformer. The sensors enabled us to determine whether the equipment was energized or not. Since the signal obtained from the sensor was very small, it was first amplified before it was fed to the Arduino microcontroller. Fig. 10 shows the circuit that was used to amplify the signal from the current sensor. As it can be seen, the output pin is pulled HIGH when no current is detected. The sensor readings are thereafter forwarded to the LoRa gateway after a time-stamp and the GPS coordinates expressed as a combination of latitude and longitude are appended. The time stamp is obtained from the Real Time Clock (RTC), and the GPS receiver supplies the GPS coordinates, both of which are attached to the Arduino MEGA 2560. Fig. 11 presents the schematic diagram of the embedded electronic monitoring device (EEMD). Fig. 12 illustrates the block diagram of the EEMD, and Fig. 13 is a photo of the assembled EEMD. In order to protect the EEMD from external elements, it was placed inside a protective waterproof casing as shown in Fig. 14.

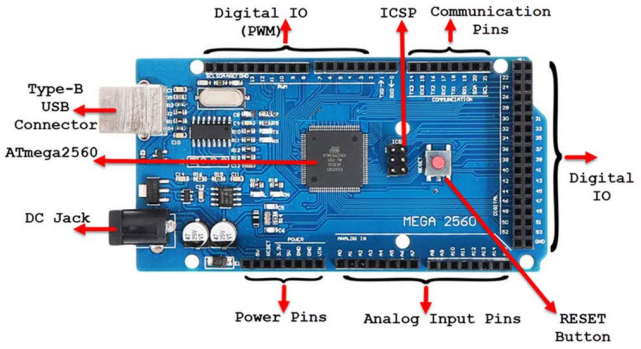

FIGURE 9. Arduino MEGA 2560 microcontroller.

3) SOLAR ENERGY HARVESTING

The battery lifetime of an embedded device has been cited as being its most significant criterion [89]. Considering that the IoT device will be deployed in the field in a remote location to continuously monitor the electrical system, there is a need to eliminate the need for regular maintenance, particularly the necessity for energy replenishment. We therefore built the monitoring device to harvest its own energy from the environment and store it in a rechargeable battery. With the generous insolation available of about 5-7 peak sunshine hours daily, resulting in about 4-6 kWh/m^2, the choice of solar is reasonable [90], [91]. A monocrystalline solar panel, the charge controller TP 4026, and a Nickel Metal Hydride (NiMH) battery were selected as shown in Fig. 15. The solar panel is a 6V/3.5W and the battery chosen is a 4.8V with a

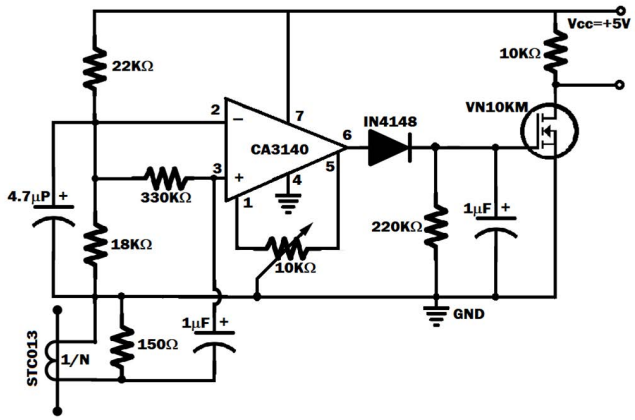

FIGURE 10. Current transformer connection and interfacing circuitry.

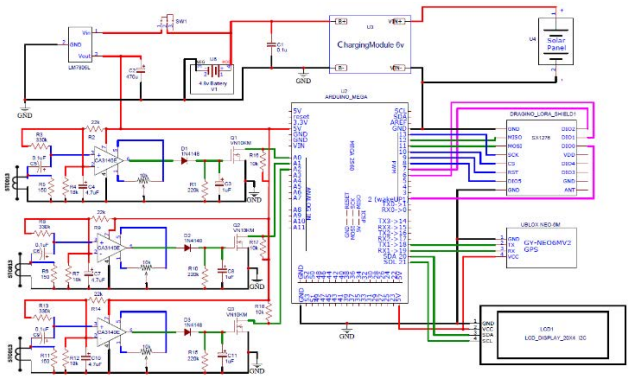

FIGURE 11. Schematic diagram of the embedded electronic monitoring device.

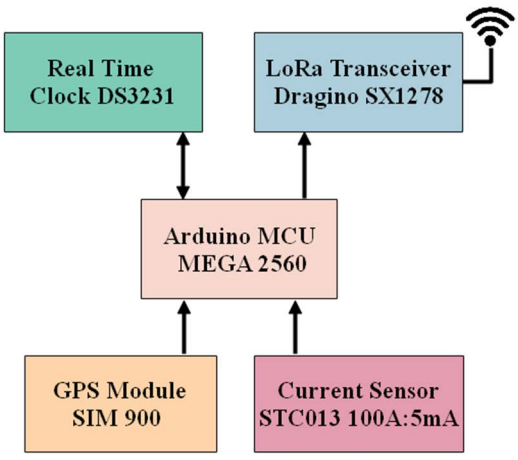

FIGURE 12. Assembly of the EEMD using Arduino MEGA 2560.

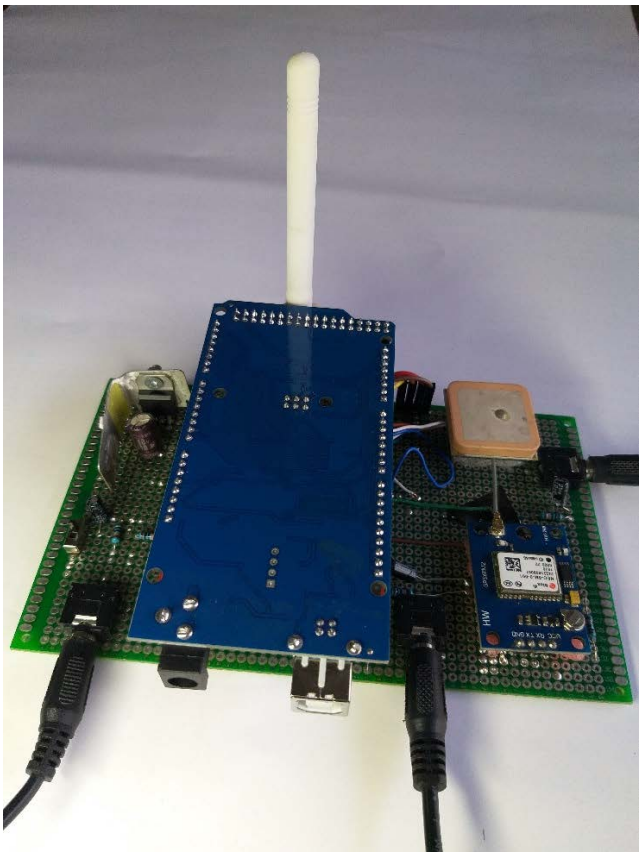

FIGURE 13. The electronic monitoring device with an Arduino board and LoRa transmitter module.

FIGURE 14. An EEMD encapsulated in a waterproof protective casing.

current-ampere hour rating of 2500mAh. These components were assembled as shown in Fig. 16. The TP 4026 charge controller boosts the voltage to 5V through an inbuilt DC-to-DC voltage booster.

The data sheet of the Arduino MEGA 2560 recommends a supply voltage of between 7V and 12V [92]. However, when this voltage is supplied through the barrel connector, it goes through a linear voltage regulator that reduces it to the 5V that is used by the microcontroller unit. This linear voltage reduction by the regulator is wasteful because voltages in excess of 5V are not put to any good use but are merely dissipated in the form of heat [93]. With the objective of maximizing the available power in mind, we decided to supply the MCU with

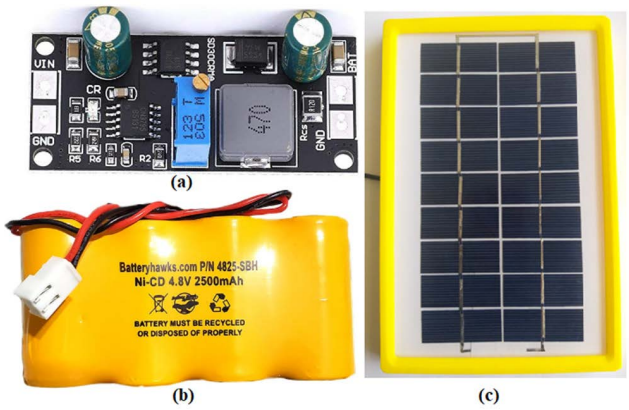

FIGURE 15. Solar energy recharge Kit (a) The charger controller (b) The battery (c) The solar panel.

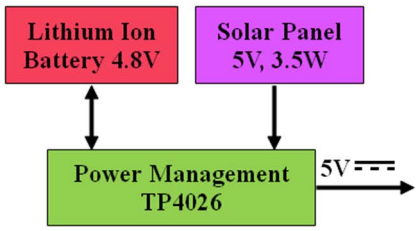

FIGURE 16. A block diagram of the solar recharging circuit.

a constant 5V input. Hence, the regulated 5V from the charge controller (TP 4026) was fed directly to the MCU through the 5V pin. This arrangement eliminated the need for the linear voltage regulator and saved the energy that would otherwise have been lost through it.

The charge controller TP4026 uses the Power Point Tracking (PPT) technique and therefore attains high efficiency. Furthermore, the DC-to-DC voltage boost converter not only maintains the voltage constant at 5V but also eliminates the need to tap energy directly from the battery terminals. PPT charge controllers exhibit critical advantages over Pulse Width Modulation (PWM) charge controllers. They not only keep the battery from overcharging, but they also boost performance by more than 30% [56], [94], [95].

4) CHARGING TIME OF THE BATTERY

In order to determine if the selected solar panel will maintain the battery in a charged condition, we calculate how much time it would take to fully recharge the battery. First, we obtain the maximum charge current using the formula shown in (4). The maximum charge current is found to be 729 mA. To cater for system losses estimated to be about (20%) and charge controller efficiency of 75%, the effective charging current, C_{eff}, is determined to be 437.5 mA using (5).

$$C_i = {}^{W}/_{V} \tag{4}$$

$$C_{eff} = {}^{W}/_{V} \times (1 - 80\%) \times 75\% \tag{5}$$

where W is the total wattage of the solar panels (3.5W) and V is the battery voltage (4.8V). To cater for inefficiencies in the charging system, a higher battery capacity is assumed and calculated using (8). A battery charge efficiency of 85% is taken, and a new value for the battery charge is obtained using (6).

$$B_c = C_c \times (85\%)^{-1} \tag{6}$$

where B_c is the battery charge capacity and C_c the rated capacity. With C_c being 2500mAh, B_c is determined to be 2941mAh. To determine how much time it would take to charge the battery, (7) was used.

$$t_\tau = {}^{B_c}/_{C_{eff}} \tag{7}$$

where t_τ is the time it takes to fully charge the battery, B_c is the battery charge capacity, and C_{eff} is the effective charging current. Using (9), the total time to fully charge (t_τ) is calculated to be 6 hours and 43 minutes. This figure assumes that the battery is fully discharged and that there are no cloudy episodes during the day. However, in reality, the battery is never used until it is completely discharged. Moreover, many batteries have built-in safety limits that, when reached, will automatically trigger a shutdown in order to protect the battery.

5) THE CLOUD SERVER AND DATA VISUALIZATION

The loss of power on a network segment is an emergency that must be promptly addressed. The platform was therefore set to trigger an alarm at the monitoring and control center. In addition, email and text messages were sent to a preselected email. The power system operator would then be able to send personnel to correct the existing anomaly. The monitoring dashboard showed the GPS location of the transformer, the status of each of the monitored phases of the transformer, and the time the fault was detected. The dashboard is shown in Fig. 17. Fig. 18 shows how the fleet of monitoring devices was deployed on the distribution network.

III. EXPERIMENTAL EVALUATION AND TEST RESULTS

The experimental findings of the deployment of the EEMDs are reported in this section. The end nodes were assembled; the sketch was compiled and uploaded into the microcontroller through the IDE. The Things Network (TTN) Stack LoRaWAN server stack was set up to receive data from the end-nodes. For visualization, the data was sent to Cayenne, which is an online dashboard for IoT applications. A data format conversion was necessary for Cayenne to receive data received from TTN. Cayenne enabled the creation of a trigger so that whenever a power outage occurred, an alarm condition was created at the monitoring and control center.

A. PLATFORM DEPLOYMENT

The LoRa-based distribution transformer-monitoring platform was piloted between August 7 and September 24, 2021. Six distribution transformers owned and operated by the

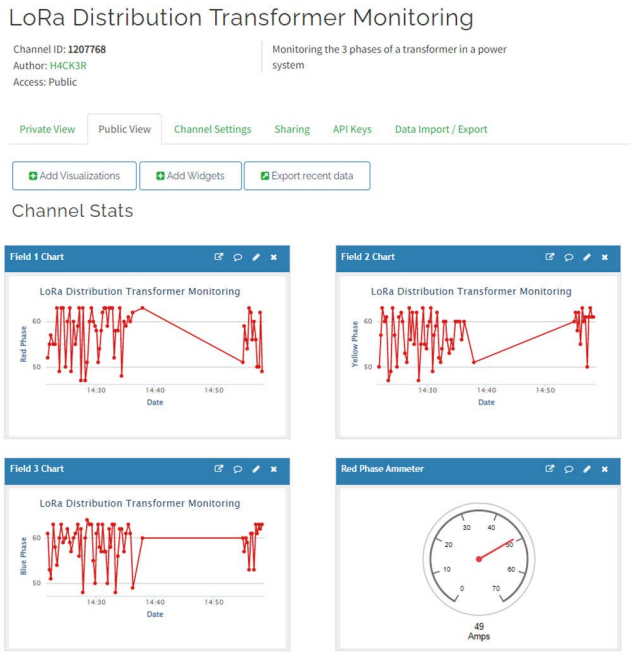

FIGURE 17. Visualization dashboard of distribution transformer monitoring.

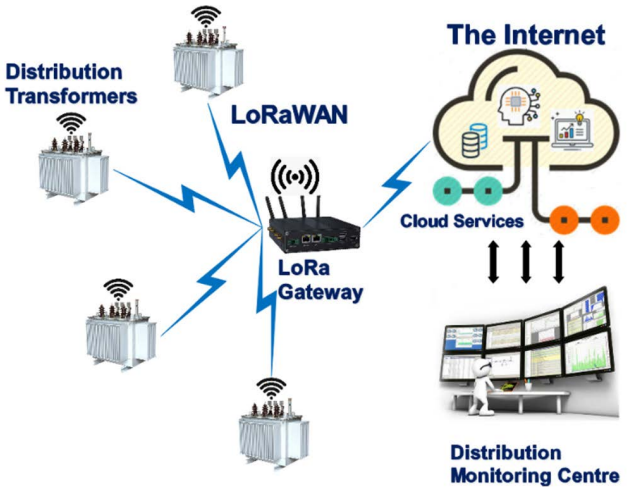

FIGURE 18. Sensor monitoring on the distribution transformers.

Kenya Power Company were used for piloting. The transformers themselves were the outdoor pole-mounted types that were suspended approximately 10 feet above the ground. Fig. 19 is a picture of the current sensors and the EEMD attached to a distribution transformer, while Fig. 20 is a satellite map showing the various locations where the specific transformers were located in the area of study. Six EEMDs were installed, one on each distribution transformer, and were set up to communicate with a centralized LoRa gateway. The gateway was placed on the fifth floor of a storied building and was positioned close to a window. It was

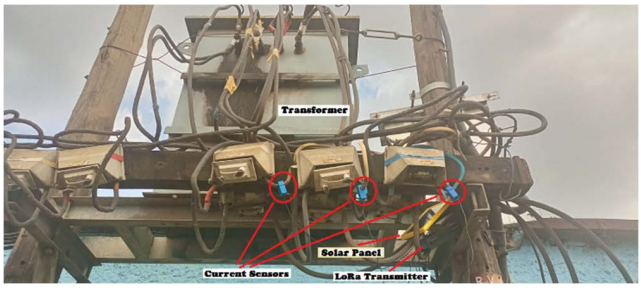

FIGURE 19. A picture showing the attachment of current sensors clamped to a distribution transformer.

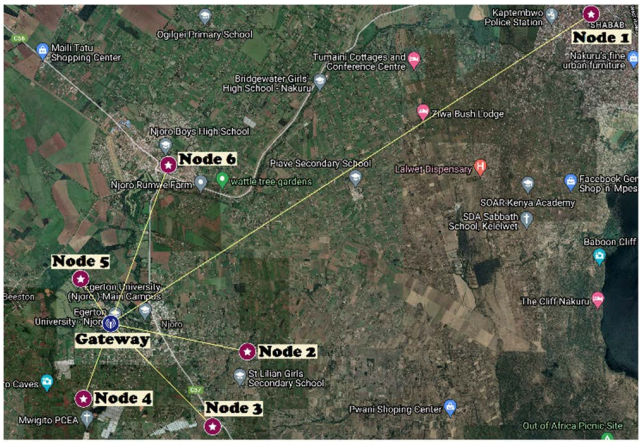

FIGURE 20. A diagram showing the location of transformers and displacement of the EEMDs from the LoRa gateway.

TABLE 2. Dispersion of the sensors from the gateway.

SENSOR ID	GPS COORDINATES	DISTANCE (m)
Node 1	-0.29361, 36.05396	16133
Node 2	-0.37908, 35.96695	3647
Node 3	-0.39804, 35.95815	3744
Node 4	-0.39098, 35.92549	1991
Node 5	-0.36067, 35.92477	1452
Node 6	-0.3318, 35.94698	4939

connected to the local Ethernet and powered by electricity via a 12V AC-DC adaptor.

The embedded electronic monitoring devices were dispatched to the various preselected transformers within the study area, with varying intervening distances between the nodes and the gateway as shown in Table 2.

B. DATA COLLECTION AND MESSAGE PAYLOAD

The data collected by the embedded electronic monitoring devices comprised the GPS location information expressed as longitude and latitude, a time-stamp, and the current reading of each phase of the transformer. In order to keep the payload small, the timestamp was trimmed to exclude the seconds. This also enabled the LoRa packets generated to conform to the LoRaWAN specifications. This information was then

TABLE 3. LoRaWAN parameter settings.

LoRaWAN Settings		
Parameter	Value	Details
Frequency	EU863-870	Class A
BW	125kHz	Default Configuration
CR	4/6	Coding rate value
SF	{7, 8, 9, 10, 11, 12}	ADR
Tx Payload Size	22 bytes	Used with SF selected

packaged into a single data structure that enabled us to send different pieces of information as one solitary payload. The total size of the LoRaWAN packet payload was calculated to be 22 bytes, including a 13-byte LoRa packet overhead. Fig. 21 shows the various parts of a LoRaWAN packet.

Table 3 shows the parameters and their settings as they have been used in this study, and Table 4 is a subset of the data collected during experimentation.

C. LoRaWAN CONFIGURATION AND PERFORMANCE

According to the LoRaWAN documentation, there are several parameters whose values can be set to ensure optimum performance. These parameters are the bandwidth, the coding rate, and the spreading factor. Since the EEMDs are fixed to a stationary point, ADR, or adaptive data rate, was enabled. ADR is an algorithm that accesses the link quality and, based on this assessment, determines the optimal SF. Thus, ADR dynamically and autonomously increases or decreases the data rate to ensure the data rate is optimal. For Forward Error Correction (FEC), a coding rate of 4/6 was chosen because it results in maximum data transfer per packet. The bandwidth was set at 125 kHz because it affords the media the highest sensitivity. Receiver sensitivity, expressed in dB, is a measure of the minimum signal strength detectable by a receiver. For best results, this quantity should ideally be of very low value. The receiver sensitivity (S) is obtained using (8).

$$S = TN + 10 \cdot log_{10}(BW) + NF - SNR_{limit} \tag{8}$$

where TN stands for thermal noise (in decibels), BW stands for bandwidth, NF stands for noise factor, and SNR_{limit} stands for the signal-to-noise ratio in decibels.

In order to assess how LoRaWAN performs, a series of packets were sent from each of the nodes (1 to 6) and the average values of the Received Signal Strength Indicator (RSSI), the Packet Reception Rate (PRR), and the Time of the Air (ToA) were recorded. For Node 1, however, no reception was possible at the gateway. These observations are summarized in Table 5.

D. BATTERY DEPLETION TIME

Energy self-sustenance is a critical aspect to the success of this work. The EEMD described in this work must, of necessity, be able to operate for many years and not be incapacitated by the depletion of power from the battery. In an effort

TABLE 4. Experiment sample data from test sites.

	Date-Time	GPS Location	I_Y, I_B, I_R	PDT
1	07-08-21 08:12	-0.39804, 35.95815	58,59,52	100.18
2	07-08-21 08:27	-0.39098, 35.92549	54,62,61	98.53
3	07-08-21 08:40	-0.3318, 35.94698	60,57,63	104.64
4	07-08-21 10:23	-0.37908, 35.96695	61,54,53	97.68
5	07-08-21 14:54	-0.36067, 35.92477	63,55,62	96.42
6	08-08-21 08:48	-0.39804, 35.95815	54,59,58	99.12
7	08-08-21 08:57	-0.36067, 35.92477	48,48,50	96.29
8	08-08-21 10:34	-0.37908, 35.96695	59,58,60	100.80
9	08-08-21 11:45	-0.39098, 35.92549	57,49,62	96.75
10	08-08-21 19:20	-0.3318, 35.94698	58,51,63	104.48
11	09-08-21 10:12	-0.3318, 35.94698	63,59,50	104.76
12	09-08-21 13:54	-0.39098, 35.92549	60,56,63	94.06
13	09-08-21 13:57	-0.37908, 35.96695	58,57,53	94.91
14	09-08-21 15:50	-0.39804, 35.95815	63,63,60	96.99
15	09-08-21 17:38	-0.36067, 35.92477	57,60,56	92.22
16	10-08-21 11:09	-0.36067, 35.92477	44,57,52	92.30
17	10-08-21 12:53	-0.39098, 35.92549	52,63,63	98.10
18	10-08-21 15:23	-0.3318, 35.94698	53,57,57	104.92
19	10-08-21 15:25	-0.37908, 35.96695	63,52,59	96.46
20	10-08-21 18:02	-0.39804, 35.95815	55,57,60	97.41
21	11-08-21 09:34	-0.39804, 35.95815	63,54,54	99.68
22	11-08-21 11:53	-0.36067, 35.92477	63,62,55	90.20
23	11-08-21 13:02	-0.39098, 35.92549	59,63,58	94.14
24	11-08-21 16:18	-0.37908, 35.96695	62,60,56	97.03
25	12-08-21 09:01	-0.36067, 35.92477	54,54,59	95.24
26	12-08-21 10:23	-0.39098, 35.92549	54,,51,58	97.85
27	12-08-21 11:01	-0.39804, 35.95815	57,61,63	97.06
28	12-08-21 12:30	-0.3318, 35.94698	62,59,63	105.68
29	12-08-21 19:28	-0.37908, 35.96695	58,61,49	102.85
30	13-08-21 09:12	-0.36067, 35.92477	57,60,61	92.40
31	13-08-21 12:01	-0.39804, 35.95815	60,58,63	100.80
32	13-08-21 12:48	-0.39098, 35.92549	63,59,49	94.86
33	13-08-21 15:59	-0.3318, 35.94698	54,59,53	105.26
34	13-08-21 18:44	-0.37908, 35.96695	50,55,58	96.46
35	14-08-21 07:28	-0.36067, 35.92477	60,49,61	95.20
36	14-08-21 08:20	-0.3318, 35.94698	54,63,61	103.73
37	14-08-21 11:12	-0.39804, 35.95815	49,48,57	96.90
38	14-08-21 12:25	-0.39098, 35.92549	59,63,59	98.36
39	14-08-21 13:30	-0.37908, 35.96695	54,61,48	98.72
40	15-08-21 08:40	-0.37908, 35.96695	48,62,48	100.80
41	15-08-21 10:51	-0.3318, 35.94698	60,58,58	104.92
42	15-08-21 12:46	-0.36067, 35.92477	52,47,62	93.36
43	15-08-21 14:15	-0.39804, 35.95815	57,62,63	97.19
44	15-08-21 16:22	-0.39098, 35.92549	51,57,47	100.46
45	16-08-21 10:23	-0.3318, 35.94698	54,59,61	105.38
46	16-08-21 12:41	-0.36067, 35.92477	58,55,52	94.44
47	16-08-21 15:11	-0.39804, 35.95815	61,62,63	99.56
48	16-08-21 16:01	-0.37908, 35.96695	62,62,63	96.85
49	16-08-21 17:30	-0.39098, 35.92549	61,56,57	97.47
50	17-08-21 10:28	-0.36067, 35.92477	63,61,60	90.68
51	17-08-21 13:34	-0.39804, 35.95815	60,50,59	96.91
52	17-08-21 13:35	-0.37908, 35.96695	58,62,56	97.75
53	17-08-21 17:54	-0.39098, 35.92549	58,53,58	93.56
54	18-08-21 09:31	-0.36067, 35.92477	59,53,61	95.52
55	18-08-21 10:58	-0.39098, 35.92549	50,56,62	98.27
56	18-08-21 11:13	-0.37908, 35.96695	57,60,63	97.07
57	18-08-21 14:42	-0.39804, 35.95815	63,50,54	95.91
58	18-08-21 16:20	-0.3318, 35.94698	60,51,48	106.08
59	19-08-21 09:08	-0.37908, 35.96695	48,60,59	96.96
60	19-08-21 09:18	-0.36067, 35.92477	49,61,49	94.16
61	19-08-21 11:25	-0.39098, 35.92549	56,58,56	102.07
62	19-08-21 15:30	-0.39804, 35.95815	48,57,59	98.64
63	20-08-21 08:21	-0.3318, 35.94698	60,61,61	103.79

TABLE 4. *(Continued.)* **Experiment sample data from test sites.**

64	20-08-21 13:29	-0.39098, 35.92549	63,63,60	95.11
65	20-08-21 13:55	-0.39804, 35.95815	52,63,54	101.92
66	20-08-21 16:45	-0.37908, 35.96695	63,59,57	100.46
67	20-08-21 19:02	-0.36067, 35.92477	47,62,47	93.46
68	21-08-21 09:22	-0.3318, 35.94698	62,60,60	103.42
69	21-08-21 11:57	-0.39804, 35.95815	62,59,63	99.88
70	21-08-21 14:52	-0.3318, 35.94698	61,53,56	106.63
71	21-08-21 15:47	-0.36067, 35.92477	59,63,51	92.58
72	21-08-21 16:39	-0.39098, 35.92549	63,51,58	98.90
73	21-08-21 17:30	-0.37908, 35.96695	50,63,63	99.08

TABLE 5. **Performance of the LoRa transmissions from test sites.**

NODE ID	PRR (%)	MEAN RSSI (dBm)	MEAN TOA (ms)
Node 1	0	n/a	n/a
Node 2	88.7	-102.6	99.25
Node 3	88.2	-92.9	98.21
Node 4	96.9	-79.1	97.47
Node 5	98.4	-77.8	94.34
Node 6	87.6	-123.2	104.91

to guarantee longevity, the system was built with the ability to replenish its own power by harvesting solar energy from the environment. This is a critical factor for IoT systems because many of these devices are deployed in far-flung areas that are also hard to reach.

It is also imperative to determine how long the battery will last while continuously powering the EEMD, assuming that there is no replenishment energy to the battery. This will give us an indication as to whether the capacity of the chosen battery is sufficient. The time it would take to completely deplete the battery power source largely depends on the rate at which current is drawn from the battery. In addition, as described earlier, the EEMD spends most of its operational life in the deep sleep mode. Due to the low duty cycle of a LoRa send operation, the EEMD is 99.9% of the time in deep sleep. For this reason, the researchers decided to estimate the life of the battery from only the power consumed during the sleep mode. This does not refute the fact that some power is consumed during the awake state, but rather is an appreciation of the fact that the power consumption when the device is ''awake'' is infinitesimal in comparison to the deep-sleep power consumption.

The life of a rechargeable battery is estimated from its rated capacity in Ampere Hours (Ah). Using a Fluke 117 digital multimeter, it was determined that the Arduino ATMEGA 2560 used about 29.13 mA when in ''Deep Sleep'' mode. The interface circuit for the current sensor draws about 5.618 mA. The current consumption during the deep sleep mode for the rest of the components of the EEMD has been extracted from their data sheets and summarized in Table 6.

Table 6 shows that the total current drawn by the EEMD in deep sleep mode is 36.4 mA. Using (9), and with a battery with a charge capacity of 2500 mAH, the battery can sustain the EEMD for about 68.65 hours, or 2 days, 20 hours, and 38 minutes. Since the battery can be fully recharged in 6 hours, we conclude that the battery capacity is sufficient for the proposed application.

TABLE 6. **Current consumption in the deep sleep state.**

COMPONENT	CURRENT
Arduino MEGA 2560 Rev3	29.13 mA
LoRa Shield SX1278	215 nA
GSM/GPRS SIM900 Module	1.5mA
Sensor Interface Circuit	5.618 mA
Real Time Clock DS3231	170µA

TABLE 7. **Comparison of the currently used fault notification system to the proposed IoT-based platform.**

METHOD	AVERAGE TIME
Telephone notification by customers	200 minutes
IoT-based Platform	0.002 minutes

$$B_{life} = {B_{cap}}/{I_{cur}} \tag{9}$$

where B_{life} is the battery life, B_{cap} is the rated battery capacity, and I_{cur} is the load current.

IV. DISCUSSION

The LPWAN is the principal component of the wide area-monitoring platform espoused in this work. Six nodes were deployed in the study area to monitor actual transformers owned and operated by Kenya Power Company Plc. Since the percentage of time the system is available is far greater than the periods of non-availability, a lot of time would have been taken to gather the necessary data for analysis. Hence, we recreated a fault at each site being monitored by isolating the current sensor using a switch so that no input is received by the microcontroller. When the current transformer is isolated, there is no input current to the op-amp CA3140 shown in Fig. 10, and this will automatically trigger a LoRa uplink transmission. This is the usual behavior of the circuit when a de-energization of the transformer occurs. In addition, the Arduino was programmed to read from the current sensors every 30 minutes for testing purposes. Cumulatively, by this arrangement, we sent about 400 LoRa packets from every node, each packet representing a fault manifestation. Data was received from all the nodes (2, 3, 4, 5, and 6) except node 1, where the PRR was zero in spite of the best efforts of the researchers to establish communication. In order to demystify this failed attempt, the researchers took the trouble of calculating the Fresnel zone between node 1 and the gateway. The Fresnel zone is an invisible, three-dimensional oval volume of the atmosphere surrounding the straight path connecting the gateway and the end node. Anything lying within this invisible volume, be it a hilltop, a building, a tree, or even the earth's surface, creates an obstacle that can attenuate the transferred signal, even if there exists a direct line of

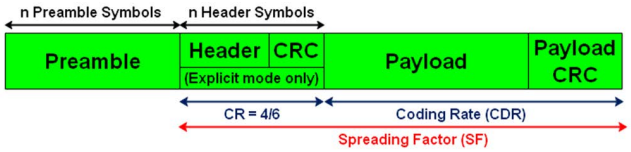

FIGURE 21. LoRaWAN packet format.

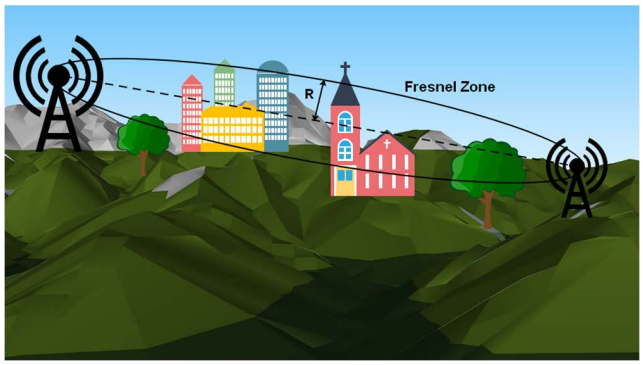

FIGURE 22. The fresnel zone with several obstacles along the transmission path.

sight between two communicating devices. To determine how big this Fresnel zone is, we used (10). R is calculated at half the distance between node 1 and the gateway. From Table 2, it is seen that the distance between the LoRa gateway and the transmitting node is 16.1 kilometers. Hence, the mid-distance is about 8.05 kilometers.

$$R = 8.657 \times \sqrt{D/f} \tag{10}$$

where R is the radius of the Fresnel zone, D is the distance, and f is the frequency. From Table 2, the distance D is seen to be 16.1 kilometers. The radius of the Fresnel zone, R, is therefore calculated to be 37.3 meters. This implies that a viable radio link between node 1 and the gateway must have a Fresnel zone with a radius of 37.3 meters midway between the devices. However, because the transmitter is located on distribution transformers that are very close to the ground, it was impossible to achieve such a Fresnel zone. The researchers therefore arrived at the conclusion that the reason the packet reception rate between Node 1 and the gateway is zero is because signal transmission is severely obstructed. As calculated above, it is expected that R should be 37.3 meters for this radio link, but given the height of the transmitter (about 10 feet), this is not possible to achieve. It was therefore concluded that the radio communication path was irreparably compromised by a combination of proximity to the ground, vegetation, and buildings, thus terminally impeding communication. As a result of this, it is observed that for objects close to the ground, and especially when it is not possible to elevate the transmitter any further, the distance between the gateway and the transmitting node should be kept at no greater than five kilometers. This is consistent with observations made in [83].

TABLE 8. Abbreviations and explications.

ACRONYM	EXPLICATION
ADR	Adaptive Data Rate
ANFIS	Adaptive Neurofuzzy Inference System
CDR	Coding Rate
CPR	Chirp Rate
CSS	Chirp Spread Spectrum
CT	Current Transformer
dB	Decibel
DR	Data Transmission Rate
EEMD	Embedded Electronic Monitoring Device
FLC	Fuzzy Logic Controller
GPRS	General Packet Radio Service
GPS	Global Positioning System
IDE	Integrated Development Environment
IoT	Internet of Things
IP	Internet Protocol
KP	Kenya Power Company Limited
L-G	Line to Ground fault
L-L	Line to Line fault
LL-G	Double Line to ground fault
L-L-L	Line to Line to line fault
L-L-L-G	Line to Line to ground fault
LoRa®	Long Range
LoRaWAN®	LoRa Wide Area Network
LTE-M	Long Term Evolution for Machines
LV	Low Voltage
MAC	Media Access Control
MCU	Microcontroller unit
MQTT	Message Queuing Telemetry Transport
MV	Medium Voltage
NB-IoT	Narrowband-IoT
NiMH	Nickel Metal Hydride
OpenWRT	Open wireless router
PDC	Phasor Data Concentrators
PDS	Power Distribution System
PDT	Packet Delivery Time
PLC	Programmable Logic Controller
PMU	Phasor Measurement Units
PoE	Power-over-Ethernet
PPT	Power Point Tracking
PRR	Packet Reception Rate
PSO	Power System Operator
PT	Potential Transformer
PV	Photovoltaic
PWM	Pulse Width Modulation
RF	Radio Frequency
RPMA	Random Phase Multiple Access
RSSI	Received Signal Strength Indicator
RTC	Real-time Clock
SCADA	Supervisory Control and Data Acquisition
SDN	Software-Defined Networking
SF	Spreading Factor
SG	Smart Grid
SNR	Signal-to-Noise Ratio
SSA	Sub-Saharan Africa
ToA	Time over the Air
TTN	The Things Network
WAN	Wide Area Network
WSN	Wireless Sensor Network

The earth's surface was itself within this zone, yet it was not physically possible to raise the antenna any further than ten feet because the distribution transformers are usually placed at that height, suspended on poles. Fig. 22 shows a

Fresnel zone with several obstacles in its path. This is the probable situation that was experienced with node 1. Even though the gateway was positioned on the fifth floor of a building complex within the study location, this was not sufficient for a transmitter placed very close to the ground and located 16 kilometers away. Despite the fact that LoRa can communicate with transmitters 1000 kilometers away, Fresnel zone clearance remains a challenge. As the distance increases, the Fresnel zone gets fatter, particularly at its mid-distance. For these long distances, it is inevitable that one uses antennas hoisted high above the ground to achieve meaningful communication. Furthermore, the formulae for computing the Fresnel zone do not take into account the curvature of the earth's surface. Therefore, for long-range radio communication technologies, the Fresnel zone clearance remains a significant factor to be considered in the establishment of a viable radio link. For the rest of the nodes, a large proportion of the packets sent arrived at the gateway without error and with a packet reception rate greater than 88%. These findings agree with those of other researchers [68], [96], [97]. This was achieved with a spreading factor of 7, a coding rate of 4/6, and a bandwidth of 125 KHz. This tells us that for the other nodes, the Fresnel zone was clear or not encroached upon to the extent of impeding all communication. The height at which the gateway was placed also contributed to the establishment of a feasible line-of-sight between the communicating devices.

Unlike in the current setup where faults are located by physically patrolling the length of the distribution cable in the area where a fault is suspected, the proposed method is not only efficient but drastically reduces the duration between the fault occurrence and the receipt of information on the incident at the monitoring and control centre. The prompt receipt of notification of a fault by the monitoring and control centre enables immediate commencement of reparative activities, resulting in shortened durations of power outages witnessed on the distribution network. This not only has the tangible effect of encouraging economic activity but also enables the power system operator to comply with regulatory demands on quality of service provision. The proposed system will also result in consumer contentment and satisfaction. Table 6 compares the existing method to the proposed platform in terms of the time taken to notify the Monitoring and Control Centre of the occurrence of a failure. The table shows that the proposed IoT-based platform reduces the time to notify the Monitoring and Control Centre by a factor of 100,000. In addition, it minimizes the time taken by the service crew to locate the faulty site since the GPS location of the EEMD is transmitted as well.

V. CONCLUSION AND FUTURE WORK

As a proof-of-concept, a LoRa-based smart fault detection and monitoring platform for the power distribution system is proposed in this work. The system with energy self-reliance capability consisted of three parts: the sensor network, the power harnessing, and data analysis. The batteries are recharged by a monocrystalline solar panel that powers the platform. The platform successfully reduces the time it takes the power system operator to become aware of a de-energization in the distribution network from several hours to only about 100 ms. This drastic reduction in the time-to-notification will play a major role in the reduction of blackout durations since it enables the PSO to immediately commence power restoration activities.

We advocate the adoption of LoRaWANs for monitoring, detecting, and finding faulted segments in the power distribution grid. Specifically, we recommend the adoption of the LoRa® technology. In the LPWAN space, LoRaWAN has projected itself as having the ability to transmit data to far-flung and remote places using low bandwidth, little energy, and high accuracy. Due to its superior resistance to noise, LoRaWAN technology is a game changer as far as long-range data transmission is concerned. This successful deployment of a LoRaWAN for the monitoring and discovery of faulted network segments in the existing legacy distribution grid demonstrates that the monitoring can be done in a cost-effective manner using low-priced hardware. Furthermore, this technique imbues the grid with feedback mechanisms and enables the power system operator to address promptly and quickly the incidences that arise on the network. This route circumvents the other, more costly alternatives that would, for instance, demand a complete overhaul of the existing system. This is a viable option for countries in the sub-Saharan Africa (SSA) region where budgetary constraints and cost prohibitions limit further enhancements to the existing electricity network.

In the future, the study may be extended to determine new and innovative ways of extending the life of the battery by reducing the current consumed by the EEMD. This may also involve fiddling with the LoRa parameters, viz., the coding rate, spreading factor, and bandwidth, to determine their effect in achieving reduced power consumption.

ACKNOWLEDGMENT

The authors express their deep gratitude to the management and staff of Kenya Power PLC, who graciously granted access to the equipment that made this study possible and further supported this work to the utmost extent possible. Further gratitude is extended to everyone who spared time to review, proofread, and edit this work.

REFERENCES

[1] N. A. Hidayatullah, A. C. Kurniawan, and A. Kalam, "Power transmission and distribution monitoring using Internet of Things (IoT) for smart grid," *IOP Conf. Ser., Mater. Sci. Eng.*, vol. 384, no. 1, 2018, Art. no. 012039, doi: 10.1088/1757-899X/384/1/012039.

[2] D. Baimel, S. Tapuchi, and N. Baimel, "Smart grid communication technologies- overview, research challenges and opportunities," in *Proc. Int. Symp. Power Electron., Electr. Drives, Autom. Motion (SPEEDAM)*, Jun. 2016, pp. 116–120, doi: 10.1109/SPEEDAM.2016.7526014.

[3] A. Sallam and O. Malik, "Microgrids and smart grids," in *Electric Distribution Systems*, 2nd ed. Boca Raton, FL, USA: Wiley, 2019, pp. 553–580, doi: 10.1002/9781119509332.CH20.

[4] Y. Saleem, N. Crespi, M. H. Rehmani, and R. Copeland, "Internet of Things-aided smart grid: Technologies, architectures, applications, prototypes, and future research directions," *IEEE Access*, vol. 7, pp. 62962–63003, 2019, doi: 10.1109/ACCESS.2019.2913984.
[5] J. Yuan, J. Shen, L. Pan, C. Zhao, and J. Kang, "Smart grids in China," *Renew. Sustain. Energy Rev.*, vol. 37, pp. 896–906, Sep. 2014, doi: 10.1016/j.rser.2014.05.051.
[6] F. H. Malik and M. Lehtonen, "A review: Agents in smart grids," *Electr. Power Syst. Res.*, vol. 131, pp. 71–79, Feb. 2016.
[7] A. Parejo, E. Personal, D. Larios, J. Guerrero, A. García, and C. León, "Monitoring and fault location sensor network for underground distribution lines," *Sensors*, vol. 19, no. 3, p. 576, Jan. 2019, doi: 10.3390/S19030576.
[8] G. Odongo, R. Musabe, and D. Hanyurwimfura, "A multinomial DGA classifier for incipient fault detection in oil-impregnated power transformers," *Algorithms*, vol. 14, no. 4, p. 128, Apr. 2021, doi: 10.3390/A14040128.
[9] G. Rigatos, "Condition monitoring of the electric power transmission and distribution system," in *Intelligent Renewable Energy Systems*. Cham, Switzerland: Springer, 2016, pp. 463–505, doi: 10.1007/978-3-319-39156-4_10.
[10] J. Taneja, "Measuring electricity reliability in Kenya," *Energy Policy*, vol. 12, p. 6, Jul. 2018, doi: 10.3403/30077701.
[11] S. Jamali, A. Bahmanyar, and E. Bompard, "Fault location method for distribution networks using smart meters," *Measurement*, vol. 102, pp. 150–157, May 2017, doi: 10.1016/j.measurement.2017.02.008.
[12] P. Nduhuura, M. Garschagen, and A. Zerga, "Impacts of electricity outages in urban households in developing countries: A case of Accra, Ghana," *Energies*, vol. 14, no. 12, p. 3676, Jun. 2021, doi: 10.3390/EN14123676.
[13] M. Takase, R. Kipkoech, and P. K. Essandoh, "A comprehensive review of energy scenario and sustainable energy in Kenya," *Fuel Commun.*, vol. 7, Jun. 2021, Art. no. 100015, doi: 10.1016/j.jfueco.2021.100015.
[14] D. Owiro, G. Poquillon, K. S. Njonjo, and C. Oduor. (2021). *Situational Analysis of Energy Industry, Policy and Strategy for Kenya. Institute of Economic*. Institute of Economic Affairs (IEA). Nairobi, Kenya. [Online]. Available: https://ieakenya.or.ke/download/situational-analysis-of-energy-industry-policy-and-strategy-for-kenya/
[15] A. K. Al Mhdawi and H. S. Al-Raweshidy, "A smart optimization of fault diagnosis in electrical grid using distributed software-defined IoT system," *IEEE Syst. J.*, vol. 14, no. 2, pp. 2780–2790, Jun. 2020, doi: 10.1109/JSYST.2019.2921867.
[16] T. Hilorme, L. Sokolova, O. Portna, L. Lysiak, and N. Boretskaya, "Smart grid concept as a perspective for the development of Ukrainian energy platform," *IBIMA Bus. Rev.*, vol. 2019, pp. 1–13, Sep. 2019, doi: 10.5171/2019.923814.
[17] S. A. A. Hakeem, A. A. Hady, and H. W. Kim, "RPL routing protocol performance in smart grid applications based wireless sensors: Experimental and simulated analysis," *Electronics*, vol. 8, no. 2, pp. 1–23, 2019, doi: 10.3390/ELECTRONICS8020186.
[18] T. Baležentis and D. Štreimikienė, "Sustainability in the electricity sector through advanced technologies: Energy mix transition and smart grid technology in China," *Energies*, vol. 12, no. 1142, pp. 1–21, 2019, doi: 10.3390/EN12061142.
[19] R. Kappagantu and S. A. Daniel, "Challenges and issues of smart grid implementation: A case of Indian scenario," *J. Electr. Syst. Inf. Technol.*, vol. 5, no. 3, pp. 453–467, Dec. 2018, doi: 10.1016/j.jesit.2018.01.002.
[20] N. Pamuk and Y. Uyaroglu, "The fault diagnosis for power system using fuzzy Petri nets," *Przeglad Elektrotechniczny*, vol. 88, no. 7a, pp. 99–102, 2012.
[21] Z. Y. He, J. W. Yang, Q. F. Zeng, and T. L. Zang, "Fault section estimation for power systems based on adaptive fuzzy Petri nets," *Int. J. Comput. Intell. Syst.*, vol. 7, no. 4, pp. 605–614, Jul. 2014, doi: 10.1080/18756891.2014.960259.
[22] M. Tan, J. Li, S. Zhao, and X. Cheng, "Method of power grid fault diagnosis using intuitionistic fuzzy Petri nets with inhibitor arcs," in *Proc. IEEE 8th Data Driven Control Learn. Syst. Conf. (DDCLS)*, May 2019, pp. 568–573, doi: 10.1109/DDCLS.2019.8908886.
[23] J. Sun, S.-Y. Qin, and Y.-H. Song, "Fault diagnosis of electric power systems based on fuzzy Petri nets," *IEEE Trans. Power Syst.*, vol. 19, no. 4, pp. 2053–2059, Nov. 2004, doi: 10.1109/TPWRS.2004.836256.
[24] S. Adhikari, N. Sinha, and T. Dorendrajit, "Fuzzy logic based on-line fault detection and classification in transmission line," *SpringerPlus*, vol. 5, no. 1, pp. 1–14, Dec. 2016, doi: 10.1186/S40064-016-2669-4.
[25] A. J. Lekie, D. C. Idoniboyeobu, and S. L. Braide, "Fault detection on distribution line using fuzzy logic," *Int. J. Sci. Eng. Res.*, vol. 9, no. 12, pp. 490–503, 2018.
[26] S.-W. Min, J.-M. Sohn, J.-K. Park, and K.-H. Kim, "Adaptive fault section estimation using matrix representation with fuzzy relations," *IEEE Trans. Power Syst.*, vol. 19, no. 2, pp. 842–848, May 2004, doi: 10.1109/TPWRS.2003.821036.
[27] T. Wu, G. Tu, Z. Q. Bo, and A. Klimek, "Fuzzy set theory and fault tree analysis based method suitable for fault diagnosis of power transformer," in *Proc. Int. Conf. Intell. Syst. Appl. Power Syst.*, Nov. 2007, pp. 1–5, doi: 10.1109/ISAP.2007.4441664.
[28] J. Xiao and F. Wen, "Combined use of fuzzy set-covering theory and mode identification technique for fault diagnosis in power systems," in *Proc. IEEE Power Eng. Soc. Gen. Meeting*, Jun. 2007, pp. 1–5, doi: 10.1109/PES.2007.385942.
[29] D. Thukaram, H. P. Khincha, and H. P. Vijaynarasimha, "Artificial neural network and support vector machine approach for locating faults in radial distribution systems," *IEEE Trans. Power Del.*, vol. 20, no. 2, pp. 710–721, Apr. 2005, doi: 10.1109/TPWRD.2005.844307.
[30] M. Jamil, S. K. Sharma, and R. Singh, "Fault detection and classification in electrical power transmission system using artificial neural network," *SpringerPlus*, vol. 4, no. 1, pp. 1–13, Dec. 2015, doi: 10.1186/S40064-015-1080-X.
[31] M. R. Zaidan, "Power system fault detection, classification and clearance by artificial neural network controller," in *Proc. Global Conf. Advancement Technol. (GCAT)*, Oct. 2019, pp. 1–5, doi: 10.1109/GCAT47503.2019.8978400.
[32] H.-J. Lee, D.-Y. Park, B.-S. Ahn, Y.-M. Park, J.-K. Park, and S. S. Venkata, "A fuzzy expert system for the integrated fault diagnosis," *IEEE Trans. Power Del.*, vol. 15, no. 2, pp. 833–838, Apr. 2000, doi: 10.1109/61.853027.
[33] H.-J. Cho and J.-K. Park, "An expert system for fault section diagnosis of power systems using fuzzy relations," *IEEE Trans. Power Syst.*, vol. 12, no. 1, pp. 342–348, Feb. 1997, doi: 10.1109/59.574957.
[34] Z. A. Vale and A. M. E. Moura, "An expert system with temporal reasoning for alarm processing in power system control centers," *IEEE Trans. Power Syst.*, vol. 8, no. 3, pp. 1307–1314, Aug. 1993, doi: 10.1109/59.260863.
[35] G. Xiong, D. Shi, L. Zhu, and X. Duan, "A new approach to fault diagnosis of power systems using fuzzy reasoning spiking neural P systems," *Math. Problems Eng.*, vol. 2013, pp. 1–13, May 2013, doi: 10.1155/2013/815352.
[36] F. S. Wen and C. S. Chang, "Probabilistic approach for fault-section estimation in power systems based on a refined genetic algorithm," *IEE Proc.-Gener., Transmiss. Distrib.*, vol. 144, no. 2, pp. 160–168, Mar. 1997, doi: 10.1049/IP-GTD:19970802.
[37] F. Wen, C. S. Chang, and W. Fu, "New approach to alarm processing in power systems based on the set covering theory and a refined genetic algorithm," *Electric Mach. Power Syst.*, vol. 26, no. 1, pp. 53–67, Jan. 1998, doi: 10.1080/07313569808955807.
[38] F. Wen and C. S. Chang, "A Tabu search approach to fault section estimation in power systems," *Electr. Power Syst. Res.*, vol. 40, no. 1, pp. 63–73, 1997, doi: 10.1016/s0378-7796(96)01140-6.
[39] G. Wang, Y. Liu, X. Chen, Q. Yan, H. Sui, C. Ma, and J. Zhang, "Power transformer fault diagnosis system based on Internet of Things," *EURASIP J. Wireless Commun. Netw.*, vol. 2021, no. 1, pp. 1–24, Dec. 2021, doi: 10.1186/s13638-020-01871-6.
[40] R. N. Krishna, N. Shyamsundar, and C. Venkatesan, "IoT based transmission line fault monitoring system," *Int. J. Res. Anal. Rev.*, vol. 7, no. 3, pp. 1–5, 2020, doi: 10.13140/RG.2.2.20627.91685.
[41] M. Mnati, A. Van den Bossche, and R. Chisab, "A smart voltage and current monitoring system for three phase inverters using an Android smartphone application," *Sensors*, vol. 17, no. 4, p. 872, Apr. 2017, doi: 10.3390/S17040872.
[42] M. U. Mehmood, A. Ulasyar, A. Khattak, K. Imran, H. S. Zad, and S. Nisar, "Cloud based IoT solution for fault detection and localization in power distribution systems," *Energies*, vol. 13, no. 11, p. 2686, May 2020, doi: 10.3390/EN13112686.
[43] S. Nunoo and E. K. Mahama, "Investigation into remote monitoring of power transformers using SCADA," *Int. J. Energy Eng.*, vol. 3, no. 6, pp. 213–219, Dec. 2013, doi: 10.5963/IJEE0306002.
[44] W. Liu, T. Wang, T. Zang, Z. Huang, J. Wang, T. Huang, X. Wei, and C. Li, "A fault diagnosis method for power transmission networks based on spiking neural P systems with self-updating rules considering biological apoptosis mechanism," *Complexity*, vol. 2020, pp. 1–18, Jan. 2020, doi: 10.1155/2020/2462647.

[45] H. Shabani, N. Julai, M. M. Ahmed, S. Khan, S. A. Hameed, and M. H. Habaebi, "Wireless communication techniques, the right path to smart grid distribution systems: A review," in *Proc. IEEE Student Conf. Res. Develop. (SCOReD)*, Dec. 2016, pp. 1–6, doi: 10.1109/SCORED.2016.7810047.

[46] I. Allafi and T. Iqbal, "Low-cost SCADA system using Arduino and reliance SCADA for a stand-alone photovoltaic system," *J. Sol. Energy*, vol. 2018, pp. 1–8, May 2018, doi: 10.1155/2018/3140309.

[47] A. Jain, T. C. Archana, and M. B. K. Sahoo, "A methodology for fault detection and classification using PMU measurements," in *Proc. 20th Nat. Power Syst. Conf. (NPSC)*, Dec. 2018, pp. 1–6, doi: 10.1109/NPSC.2018.8771757.

[48] V. S. B. Kurukuru, A. Haque, R. Kumar, M. A. Khan, and A. K. Tripathy, "Machine learning based fault classification approach for power electronic converters," in *Proc. IEEE Int. Conf. Power Electron., Drives Energy Syst. (PEDES)*, Dec. 2020, pp. 2002–2008, doi: 10.1109/PEDES49360.2020.9379365.

[49] *Factors Affecting PMU Installation Costs*, U.S. Dept. Energy, Washington, DC, USA, 2014.

[50] O. O. Babayomi and P. O. Oluseyi, "Intelligent fault diagnosis in a power distribution network," *Adv. Electr. Eng.*, vol. 2016, pp. 1–10, Oct. 2016, doi: 10.1155/2016/8651630.

[51] Y. Song, J. Lin, M. Tang, and S. Dong, "An Internet of Energy Things based on wireless LPWAN," *Engineering*, vol. 3, no. 4, pp. 460–466, 2017, doi: 10.1016/J.ENG.2017.04.011.

[52] A. M. Yousuf, E. M. Rochester, B. Ousat, and M. Ghaderi, "Throughput, coverage and scalability of LoRa LPWAN for Internet of Things," in *Proc. IEEE/ACM 26th Int. Symp. Quality Service (IWQoS)*, Jun. 2018, pp. 1–10, doi: 10.1109/IWQoS.2018.8624157.

[53] A. M. A. Rahman, F. H. K. Zaman, and S. A. C. Abdullah, "Performance analysis of LPWAN using LoRa technology for IoT application," *Int. J. Eng. Technol.*, vol. 7, no. 4, pp. 212–216, 2018, doi: 10.14419/IJET.V7I4.11.21387.

[54] S. Ahmed, "Realizing the benefits of energy harvesting for IoT," in *Role of IoT in Green Energy Systems*. Hershey, PA, USA: IGI Global, 2021, pp. 144–155, doi: 10.4018/978-1-7998-6709-8.CH006.

[55] S. Muzafar, "Energy harvesting models and techniques for green IoT," in *Role of IoT in Green Energy Systems*. Hershey, PA, USA: IGI Global, 2021, pp. 117–143, doi: 10.4018/978-1-7998-6709-8.CH005.

[56] S. Chalasani and J. M. Conrad, "A survey of energy harvesting sources for embedded systems," in *Proc. IEEE SoutheastCon*, Apr. 2008, pp. 442–447, doi: 10.1109/SECON.2008.4494336.

[57] T. Sanislav, G. D. Mois, S. Zeadally, and S. C. Folea, "Energy harvesting techniques for Internet of Things (IoT)," *IEEE Access*, vol. 9, pp. 39530–39549, 2021, doi: 10.1109/ACCESS.2021.3064066.

[58] A. Mindang and P. Siripongwutikorn, "Solar power prediction in IoT devices using environmental and location factors," in *Proc. 5th Int. Conf. Mach. Learn. Technol.*, Jun. 2020, pp. 119–123, doi: 10.1145/3409073.3409086.

[59] R. A. Kjellby, T. E. Johnsrud, S. E. Loetveit, L. R. Cenkeramaddi, M. Hamid, and B. Beferull-Lozano, "Self-powered IoT device for indoor applications," in *Proc. 31st Int. Conf. VLSI Design 17th Int. Conf. Embedded Syst. (VLSID)*, Jan. 2018, pp. 455–456, doi: 10.1109/VLSID.2018.110.

[60] M. Sinclair, "The Internet of Things," in *Ethical Ripples of Creativity and Innovation*. London, U.K.: Palgrave Macmillan, 2017, doi: 10.1057/9781137505545.

[61] J. A. Stankovic, "Research directions for the Internet of Things," *IEEE Internet Things J.*, vol. 1, no. 1, pp. 3–9, Feb. 2014, doi: 10.1109/JIOT.2014.2312291.

[62] O. Khutsoane, B. Isong, and A. M. Abu-Mahfouz, "IoT devices and applications based on LoRa/LoRaWAN," in *Proc. 43rd Annu. Conf. IEEE Ind. Electron. Soc.*, Oct. 2017, pp. 6107–6112, doi: 10.1109/IECON.2017.8217061.

[63] G. Gupta and R. Van Zyl, "Energy harvested end nodes and performance improvement of LoRa networks," *Int. J. Smart Sens. Intell. Syst.*, vol. 14, no. 1, pp. 1–15, Jan. 2021, doi: 10.21307/IJSSIS-2021-002.

[64] T. Bouguera, J. F. Diouris, J. J. Chaillout, R. Jaouadi, and G. Andrieux, "Energy consumption model for sensor nodes based on LoRa and LoRaWAN," *Sensors*, vol. 18, no. 7, pp. 1–23, 2018, doi: 10.3390/S18072104.

[65] V. Reddy, K. Jitesh, S. Ashif, C. V. Ravikumar, and B. Kalapraveen, "LPWAN technologies for IoT deployment," *Int. J. Electr. Eng. Technol.*, vol. 11, no. 3, pp. 285–296, 2020, doi: 10.1109/PERCOMW.2018.8480255.

[66] F. Adelantado, X. Vilajosana, P. Tuset-Peiro, B. Martinez, and J. Melia, "Understanding the limits of LoRaWAN," in *Proc. Int. Conf. Embedded Wireless Syst. Netw.*, Sep. 2016, pp. 8–12, doi: 10.1109/MCOM.2017.1600613.

[67] M. Iqbal, A. Y. M. Abdullah, and F. Shabnam, "An application based comparative study of LPWAN technologies for IoT environment," in *Proc. IEEE Region 10 Symp. (TENSYMP)*, Jun. 2020, pp. 1857–1860, doi: 10.1109/TENSYMP50017.2020.9230597.

[68] F. Turčinović, G. Šišul, and M. Bosiljevac, "LoRaWAN base station improvement for better coverage and capacity," *J. Low Power Electron. Appl.*, vol. 12, no. 1, pp. 1–11, 2022, doi: 10.3390/JLPEA12010001.

[69] M. Iqbal, A. Y. M. Abdullah, and F. Shabnam, "An application based comparative study of LPWAN technologies for IoT environment," in *Proc. IEEE Region 10 Symp. (TENSYMP)*, Jun. 2020, pp. 1–6, doi: 10.1109/TENSYMP50017.2020.9230597.

[70] A. Augustin, J. Yi, T. Clausen, and W. Townsley, "A study of LoRa: Long range & low power networks for the Internet of Things," *Sensors*, vol. 16, no. 9, p. 1466, Sep. 2016, doi: 10.3390/S16091466.

[71] E. Murdyantoro, A. W. W. Nugraha, A. W. Wardhana, A. Fadli, and M. I. Zulfa, "A review of LoRa technology and its potential use for rural development in Indonesia," in *Proc. AIP Conf.*, 2019, pp. 1–7, doi: 10.1063/1.5097480.

[72] E. Migabo, K. Djouani, A. Kurien, and T. Olwal, "A comparative survey study on LPWA networks: LoRa and NB-IoT," in *Proc. Future Technol. Conf. (FTC)*, 2017, pp. 1045–1051, doi: 10.1016/j.procs.2019.08.090.

[73] L. P. Fraile, S. Tsampas, G. Mylonas, and D. Amaxilatis, "A comparative study of LoRa and IEEE 802.15.4-based IoT deployments inside school buildings," *IEEE Access*, vol. 8, pp. 160957–160981, 2020, doi: 10.1109/ACCESS.2020.3020685.

[74] M. A. I. M. Ariff, Y. L. Then, and F. S. Tay, "Establish connection between remote areas and city to improve healthcare services," in *Proc. Int. Conf. Green Hum. Inf. Technol. (ICGHIT)*, Jan. 2019, pp. 18–23, doi: 10.1109/ICGHIT.2019.00012.

[75] K. Mekkil, "A comparative study of LPWAN technologies for large-scale IoT deployment," *ICT Exp.*, vol. 5, no. 1, pp. 1–7, 2019, doi: 10.1016/j.icte.2017.12.005.

[76] A. Samad, "A comparative study on emerging radio technologies for IoT," Jaewoo Corp., South Korea, Tech. Rep. JKL072-5472, 2020.

[77] J. C. Gambiroza, T. Mastelic, P. Solic, and M. Cagalj, "Capacity in LoRaWAN networks: Challenges and opportunities," in *Proc. 4th Int. Conf. Smart Sustain. Technol. (SpliTech)*, Jun. 2019, pp. 1–6, doi: 10.23919/SpliTech.2019.8783184.

[78] T. A. Salih and M. S. Noori, "Using LoRa technology to monitor and control sensors in the greenhouse," *IOP Conf. Ser. Mater. Sci. Eng.*, vol. 928, no. 3, 2020, Art. no. 032058, doi: 10.1088/1757-899X/928/3/032058.

[79] V. Eremin and A. Borisov, "A research of the propagation of LoRa signals at 433 and 868 MHz in difficult urban conditions," *IOP Conf. Ser., Mater. Sci. Eng.*, vol. 363, May 2018, Art. no. 012014, doi: 10.1088/1757-899X/363/1/012014.

[80] A. Raychowdhury and A. Pramanik, "Survey on LoRa technology: Solution for Internet of Things," in *Intelligent Systems, Technologies and Applications* (Advances in Intelligent Systems and Computing), vol. 1148. Singapore: Springer, 2020, doi: 10.1007/978-981-15-3914-5_20.

[81] R. Kufakunesu, G. P. Hancke, and A. M. Abu-Mahfouz, "A survey on adaptive data rate optimization in LoRaWAN: Recent solutions and major challenges," *Sensors*, vol. 20, no. 18, pp. 1–25, 2020, doi: 10.3390/S20185044.

[82] I. Cheikh, R. Aouami, E. Sabir, M. Sadik, and S. Roy, "Multi-layered energy efficiency in LoRa-WAN networks: A tutorial," *IEEE Access*, vol. 10, pp. 9198–9231, 2022, doi: 10.1109/ACCESS.2021.3140107.

[83] T. Attia, M. Heusse, B. Tourancheau, and A. Duda, "Experimental characterization of LoRaWAN link quality," in *Proc. IEEE Global Commun. Conf. (GLOBECOM)*, Dec. 2019, pp. 1–7, doi: 10.1109/GLOBECOM38437.2019.9013371.

[84] R. Liang, L. Zhao, and P. Wang, "Performance evaluations of LoRa wireless communication in building environments," *Sensors*, vol. 20, no. 14, pp. 1–19, 2020, doi: 10.3390/S20143828.

[85] M. Jung, O. Niculita, and Z. Skaf, "Comparison of different classification algorithms for fault detection and fault isolation in complex systems," *Proc. Manuf.*, vol. 19, pp. 111–118, Jan. 2018, doi: 10.1016/j.promfg.2018.01.016.

[86] A. Kaur, Y. S. Brar, and G. Leena, "Fault detection in power transformers using random neural networks," *Int. J. Electr. Comput. Eng.*, vol. 9, no. 1, pp. 78–84, 2019, doi: 10.11591/IJECE.V9I1.PP78-84.

[87] J. Davies, *The Internet of Things: From Data to Insight*. Croydon, U.K.: Wiley, 2020.
[88] I. Sahmi, A. Abdellaoui, T. Mazri, and N. Hmina, "MQTT-PRESENT: Approach to secure Internet of Things applications using MQTT protocol," *Int. J. Electr. Comput. Eng.*, vol. 11, no. 5, pp. 4577–4586, 2021, doi: 10.11591/ijece.v11i5.pp4577-4586.
[89] S. Devalal and A. Karthikeyan, "LoRa technology—An overview," in *Proc. 2nd Int. Conf. Electron., Commun. Aerosp. Technol. (ICECA)*, Mar. 2018, pp. 284–290, doi: 10.1109/ICECA.2018.8474715.
[90] *A Renewable Energy Roadmap Report*, Int. Renew. Energy Agency, Abu Dhabi, United Arab Emirates, 2015. [Online]. Available: https://www.irena.org/publications
[91] B. Albert, K. Kendagor, and R. J. Prevost, "Energy diversity and development in Kenya," *Joint Force Quart.*, vol. 70, pp. 94–99, Jan. 2013.
[92] *Arduino Mega 2560 Data Manual*, Atmel, Chandler, AZ, USA, 2015. [Online]. Available: https://www.microchip.com/
[93] Y. A. Badamasi, "The working principle of an Arduino," in *Proc. 11th Int. Conf. Electron., Comput. Comput. (ICECCO)*, Sep. 2014, pp. 1–4, doi: 10.1109/ICECCO.2014.6997578.
[94] X. Meng, X. Li, C.-Y. Tsui, and W.-H. Ki, "An indoor solar energy harvesting system using dual mode SIDO converter with fully digital time-based MPPT," in *Proc. IEEE Int. Symp. Circuits Syst. (ISCAS)*, May 2016, pp. 2354–2357, doi: 10.1109/ISCAS.2016.7539057.
[95] G. Zhou, L. Huang, W. Li, and Z. Zhu, "Harvesting ambient environmental energy for wireless sensor networks: A survey," *J. Sensors*, vol. 2014, pp. 1–20, Jun. 2014, doi: 10.1155/2014/815467.
[96] B. Myagmardulam, R. Miura, F. Ono, T. Kagawa, L. Shan, T. Nakayama, F. Kojima, and B. Choijil, "Performance evaluation of LoRa 920 MHz frequency band in a hilly forested area," *Electronics*, vol. 10, no. 4, p. 502, Feb. 2021, doi: 10.3390/ELECTRONICS10040502.
[97] O. H. Kombo, S. Kumaran, and A. Bovim, "Design and application of a low-cost, low-power, LoRa-GSM, IoT enabled system for monitoring of groundwater resources with energy harvesting integration," *IEEE Access*, vol. 9, pp. 128417–128433, 2021, doi: 10.1109/ACCESS.2021.3112519.

GEORGE Y. ODONGO (Graduate Student Member, IEEE) received the B.Sc. degree in computer science from Egerton University, Nakuru, Kenya, in 2007, and the M.Sc. degree in data communication and software engineering from Makerere University, Kampala, Uganda, in 2011. He is currently pursuing the Ph.D. degree in embedded computing systems with the African Center of Excellence in Internet of Things (ACE-IoT), College of Science and Technology, University of Rwanda.

Since early 2011, he has been a Lecturer and a Researcher at the Department of Computer Science, Egerton University. His research interests include communication technologies, the Internet of Things (IoT), computer networks, machine learning, network protocols and algorithms, and embedded computing systems. He is especially passionate about information and communication technology for development (ICT4D). He is a member of the IEEE Computer Society (ICS), the Computer Society of Kenya (CSK), the Internet Society of Kenya (ISK), and the European Alliance for Innovation (EAI).

RICHARD MUSABE received the Bachelor of Science degree in computer engineering and information technology from the Kigali Institute of Science and Technology (KIST), Rwanda, in 2006, and the master's and Ph.D. degrees in network security from Glasgow Caledonian University, Glasgow, U.K., in 2009 and 2013, respectively.

His postdoctoral studies were also in mobile communication and were completed in 2018. He is currently working as an Associate Professor and the Dean of the School of ICT, College of Science and Technology, University of Rwanda. He has contributed immensely to the education sector as both a University Senior Lecturer and a Supervisor of master's and Ph.D. students. His research interests include cellular communication, VoIP, cross-layer scheduling schemes, performance evaluation of computer systems and networks, computer network simulation, network security, the IoT, e-Health, and big data.

DAMIEN HANYURWIMFURA received the B.Sc. degree in computer engineering and information technology from the University of Rwanda (Former KIST), in 2005, and the M.Sc. and Ph.D. degrees in computer science and technology from Hunan University, China, in 2010 and 2015, respectively. He is currently working as an Associate Professor and the Director of the African Center of Excellence in the Internet of Things (ACE-IoT), College of Science and Technology, University of Rwanda.

ABUBAKAR DIWANI BAKARI received the B.Sc. degree in computing science and the M.Sc. degree in computer science from the University of Dar es Salaam (UDSM), Tanzania, in 2004 and 2010, respectively, and the Ph.D. degree from the University Putra Malaysia (UPM), in 2016. He is currently working as a Senior Lecturer and the Head of the Department of Computer Science and IT, State University of Zanzibar (SUZA), Tanzania.